Journal Pre-proof

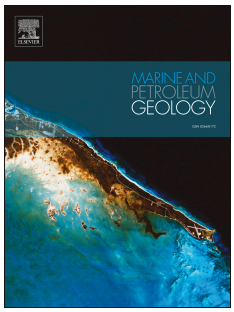

The effects of uplift and erosion on the petroleum systems in the southwestern Barents Sea: Insights from seismic data and 2D petroleum systems modelling

Dimitrios Ktenas, Jesper Kresten Nielsen, Erik Henriksen, Ivar Meisingset, Oliver Schenk

PII: S0264-8172(23)00441-5

DOI: https://doi.org/10.1016/j.marpetgeo.2023.106535

Reference: JMPG 106535

To appear in: *Marine and Petroleum Geology*

Received Date: 15 February 2023

Revised Date: 3 October 2023

Accepted Date: 4 October 2023

Please cite this article as: Ktenas, D., Nielsen, J.K., Henriksen, E., Meisingset, I., Schenk, O., The effects of uplift and erosion on the petroleum systems in the southwestern Barents Sea: Insights from seismic data and 2D petroleum systems modelling, *Marine and Petroleum Geology* (2023), doi: https://doi.org/10.1016/j.marpetgeo.2023.106535.

The effects of uplift and erosion on the petroleum systems in the southwestern Barents Sea: Insights from seismic data and 2D petroleum systems modelling

Dimitrios Ktenas[1,2*], Jesper Kresten Nielsen[3], Erik Henriksen[4,5], Ivar Meisingset[6], Oliver Schenk[7]

[1] Department of Geosciences, UiT The Arctic University of Norway, Dramsveien 201, 9037 Tromsø, Norway.

[2] Hellenic Hydrocarbon and Energy Resources Management Company S.A. (HEREMA), D. Margari 18, 11525 Athens, Greece.

[3] OKEA ASA, Kongens gate 8, 7011 Trondheim, Norway.

[4] Department of Technology and Safety, UiT The Arctic University of Norway, Campus Harstad, Havnegata 5, 9404 Harstad, Norway.

[5] Henriksen Maritime Consultancy AS, Los Holtes vei 49, 9414 Harstad, Norway.

[6] ModelGeo AS, Borgenbanken 5, 0370 Oslo, Norway.

[7] Schlumberger Aachen Technology Center, Ritterstr. 23, 52072 Aachen, Germany.

*Corresponding author. E-mail: dimitriosktenas@gmail.com

Keywords: Southwestern Barents Sea, Basin modelling, Net apparent erosion, Maximum burial depth, Petroleum systems

ABSTRACT

In the past three decades, the hydrocarbon prospectivity has been enigmatic in the southwestern Barents Sea as gas discoveries have dominated over oil. However, more recent discoveries indicate oil potential, especially in the Polheim Platform and Hoop Complex areas. Cenozoic uplift and erosion episodes are critical because they control the duration and depth of maximum burial of source rocks and the reduction of porosity of reservoir rocks due to diagenetic processes at larger depth and increased temperatures. Modelling of interpreted horizons from the southwestern Barents Sea provide a best-fit realization of the basin-scale sedimentary filling from the post-rifting in the Jurassic until the Last Glacial Maximum. 2D basin modelling was performed across one regional seismic section crossing the southwestern Barents Sea. For calibration of the 2D model, 1D modelling was performed for a selected number of wells in the region by integrating different estimates of net apparent erosion (velocity inversion of wells, interpreted profiles and structure maps as well as from temperature and vitrinite reflectance data) in order to assess the burial, thermal and maturity history of the source rocks at various well locations as well as along the 2D profile. Simulation results show that the Upper Jurassic source rock is immature to marginal mature in the central and eastern parts of the Norwegian Barents Sea. The western part is characterised by high chargeability of traps associated with rich source kitchens and porous reservoir rocks. Although not proven by commercial discoveries, there are evidences that the Permian Ørret and the Lower-Middle Triassic basal Klappmyss and basal Kobbe shales may be important gas-prone source rocks in the eastern Norwegian Barents Sea. Consequently, the exploration must rely on the Triassic and/or Palaeozoic source rocks in the eastern area.

1. Introduction

The southwestern Barents Sea represents one of the largest areas of continental shelf comprising several structural highs, platforms and basins (Fig. 1). It is surrounded by a series of well-known hydrocarbon basins, such as the Norwegian Sea, the Canadian Arctic Sverdrup Basin, the North Slope of Alaska, the Western Siberian Basin and the Timan-Pechoran Basin and hence, is an obvious target for extensive exploration activities (Spencer et al., 2011).

Since the 1980's the petroleum industry started exploration in the southwestern Barents Sea where the main targets are found in the Early Carboniferous to Tertiary interval. Since then, 138 exploration wells and 30 appraisal wells have been drilled according to the Norwegian Petroleum Directorate (NPD, 2022a). According to the exploration well record, in areas with commercial resources, like the Hammerfest Basin, Bjørnøya Basin, Hoop area and potentially Loppa High, are characterised by a high technical discovery rate (>50%). Conversely, in other locations of the Norwegian Barents Sea, sub-commercial gas discoveries were recorded, such as in the case of the discovery well 7319/12-1 Pingvin. It is worth highlighting that nearly all drilled wells in these areas have indicated the presence of hydrocarbon shows. Subsequently, recent oil and gas discoveries (e.g., Johan Castberg and the near-field exploration wells 7220/8-2 S Snøfonn Nord, 7220/8-3 Skavl Stø, 7220/7-4 Isflak, 7324/8-1 Wisting, 7324/6-1 Sputnik, 7120/1-3 Gohta, 7219/12-1 Filicudi, 7220/11-1 Alta, 7219/9-2 Kayak as well as the northernmost offshore well ever drilled in the Norwegian Barens Sea, the 7435/12-1 Korpfjell prospect; NPD, 2022a) provided optimism and revitalized interest in further exploration endeavours within the Norwegian Barents Sea region.

Dry wells, as a result of leakage and re-migration of the oil and gas in the southwestern Barents Sea, is a phenomenon closely related to the severe uplift and erosion events that have

taken place in the region (Figs. 2 and 3). The morphology and final outline of the basins and platforms are caused by several tectonic and glacial processes (Riis and Fjeldskaar, 1992; Dimakis et al., 1998; Rasmussen et al., 1998; Doré et al., 2002a; Cavanagh et al., 2006; Duran et al., 2013a; Henriksen et al., 2021, 2022). It is generally agreed that the Norwegian mainland has experienced up to 1000 m uplift and erosion (e.g., Henriksen et al., 2011a). Additionally, there is an increasing amount of erosion (up to 2500 m) towards the northern part of the Barents Shelf.

Furthermore, there is a marked decrease in erosion towards the west approaching to zero along the western Barents Sea margin (Henriksen et al., 2011a; Baig et al., 2016; Lasabuda et al., 2018; Amantov and Fjeldskaar, 2018; Ktenas et al., 2017, 2019). Along the southern flank of the Norwegian Barents Sea, the Finnmark Platform is characterized by uplift and major erosion of sequences from Carboniferous to Tertiary and this can be clearly seen as major truncation in the seismic sections (Figs. 3, 4, 5 and 6).

Understanding the burial history in sedimentary basins is a key step to determine and evaluate the hydrocarbon prospectivity. Defining the maximum burial of source rocks and their maturation, is important for constraining the time of hydrocarbon generation and expulsion from the source rocks to the time of trap formation. Severe uplift and erosion can cause source rock cooling, alteration of the reservoir rock quality, variation in migration pathways and hydrocarbon leakage and spill from traps (Doré and Jensen, 1996; Doré et al., 2002a; Cavanagh et al., 2006; Ohm et al., 2008; Henriksen et al., 2011a, 2021, 2022; Zieba and Grøver, 2016; Novoselov et al., 2018). Faults can also be re-activated and become conduits for hydrocarbon leakage to the surface (Ostanin et al., 2017; Tasianas et al., 2018; Bellwald et al., 2018a; Kishankov et al.,

2022). Further key implications that uplift and erosion can have on the petroleum systems are summarised and discussed by several authors (e.g., Doré et al., 2002a, b; Henriksen et al., 2011a; Hartz et al., 2018).

Significant research has therefore been carried out to estimate the net erosion, which in several studies is separated into several Cenozoic erosion episodes based on detailed chronostratigraphic studies in wells which clearly indicate a pre-glacial (Oligo-Miocene) and a glacial erosion event (Cavanagh et al., 2006; Anell et al., 2009; Green and Duddy, 2010; Henriksen et al., 2011a; Laberg et al., 2012; Duran et al., 2013a; Nielsen et al., 2013; 2015; Amantov and Fjeldskaar, 2018; Ktenas et al., 2017; Ostanin et al., 2017; Lasabuda et al., 2018; Ktenas et al., 2019; Iyer et al., 2021). However, the timing and magnitude of the uplift events are still poorly constrained and consequently there are still uncertainties regarding the impact on prospectivity and petroleum systems of the various episodes.

To fully understand the processes controlling petroleum charge and migration, interpreted seismic data, vitrinite reflectance and temperature data were used as input in 1D and 2D petroleum systems modelling (Clark et al., 2014; Gac et al., 2018). In the 1980s, and in particular in the last decade, starting in 2011 the main exploration focus was in the Hammerfest Basin (e.g., Snøhvit field) and past basin and petroleum systems modelling studies contributed to the implementation of the glacial cycles in 2D (e.g., Cavanagh et al., 2006; Duran et al., 2013a; Baig et al., 2016; Kishankov et al., 2022).

2D basin and petroleum systems modelling was performed along a regional seismic section crossing the southwestern Barents Sea, previously described by Ktenas et al. (2017, 2019). For calibration of the 2D model, 1D modelling was performed for a selected number of

wells in the southwestern Barents Sea (Fig. 3). Furthermore, different estimates of net apparent erosion (by velocity inversion of wells, profiles and maps as well as temperature and vitrinite reflectance) were integrated to assess and further discuss the consequences on the subsidence and thermal history of sediments.

In this study, the petroleum systems modelling of the southwestern Barents Sea shows the importance of adjusting the exploration strategy to shallower depth and lower temperatures as a consequence of severe exhumation. Improving rate of oil and gas discoveries can be achieved through the determination of locations where areas and depths are characterised by high chargeability of traps associated with rich source kitchens and porous reservoir rocks.

2. Geological background of the southwestern Barents Sea

The study area is situated in the southwestern Barents Sea bounded to the west by the continental slope of the Norwegian-Greenland Sea, from Svalbard in the north, the Russian Barents Sea to the east and to the coasts of Norway in the south (Fig. 1). The latter borderlands, represent the pre-Caledonian passive margin of Baltica. During the Ordovician and Early Devonian times, the western margin of Baltica collided with and was subducted below Laurentia resulting in regional metamorphism that formed the crystalline basement, which is underlying the southwestern Barents Sea (Torsvik et al., 2001; Roberts, 2003). Following the Caledonian orogeny which culminated approximately in ca. 400 Ma (Early Devonian), the western margin of Baltica acted as a transfer zone connecting the extensions arising in the present-day North Atlantic and Arctic regions (Doré, 1991; Torsvik et al., 2001; Clark et al., 2014; Gasser, 2014). The Caledonian basement rocks are now widely exposed and mapped in the county of Finnmark (Gernigon et al., 2014; Nasuti et al., 2015; Henriksen et al., 2021, 2022; Doré et al., 2023). Since

the late Carboniferous, several significant rifting events of basin development have occurred and contributed to the present-day configuration of the southwestern Barents Sea. Those events include the development of NE-trending half-grabens during the Late Carboniferous (e.g., the first appearance of the Hammerfest Basin and formation of the Nordkapp Basin) and unroofing of the Loppa High during the Late Permian-Early Triassic (Hendriks, 2003; Hendriks and Andriessen, 2002; Smelror et al., 2009; Gernigon et al., 2014). During the middle Triassic, to the east, salt diapiric movements are interpreted to have begun in the Nordkapp Basin (Fig. 6) (Nilsen et al., 1995; Rojo et al., 2019; Doré et al., 2023). Towards the Late Triassic, there was an apparent tectonic activity in the North Atlantic and Artic regions which continued until the early Jurassic times (Gernigon et al., 2014; Henriksen et al., 2021, 2022).

The northern progradation of the Middle Jurassic to Early Cretaceous Atlantic rifting affected mainly the western margin of the Barents Shelf (Faleide et al., 1996; Tsikalas et al., 2012), whereas the northern Barents Sea was subsequently uplifted, perhaps as a response to the opening of the Arctic Ocean, and large amounts of sediments were eroded and deposited into the deeply subsiding basins in the west (e.g., Grogan et al., 1999). The Cretaceous rifting led to subsidence as well as to the development of major deep basins such as the Harstad, Tromsø and Sørvestsnaget basins (Fig. 1). The Late Cretaceous-Late Paleocene transition marks the effect of fault-related (strike-slip movements and deformation) processes between Norway, Svalbard and Greenland. This led to the formation of pull-apart basins in the westernmost part of the Barents Sea while the Paleocene-Eocene transition (at around 55 Ma) marks the continental break-up of the North Atlantic margin and opening of the Norwegian-Greenland Sea (Faleide et al., 2008) (Fig. 2). Thick and continuous stratigraphic sequences of Paleocene and Eocene sediments are recorded in the Sørvestsnaget Basin (Fig. 3). They are bounded to the west by the volcanic margin of the Senja Fracture Zone and later they were truncated as a consequence of shallow marine conditions during the Oligocene (Ryseth et al., 2003). Since then, the southwestern

Barents Sea has undergone several and repeated phases of uplift and erosion and eroded sediments have been deposited along the western edge of the passive margin (Nyland et al., 1992). The southwestern Barents Sea was subsequently covered by thick stratigraphic sequences of preserved Paleogene and Neogene sediment deposits, which testify the occurrence of Cenozoic erosion (Fig. 3). In the late Pleistocene, widespread evidence of glacial grounding at the shelf edge shows the multiple ice-sheet advances that have occurred (Andreassen et al., 2007; Rafaelsen et al., 2007; Bellwald et al., 2018b). At this stage of evolution, the southwestern Barents Sea is characterised by significant erosion of sediments and ice loading which subsequently were followed by de-loading and uplift during deglaciation episodes (Knies et al., 2009; Nielsen et al., 2013, 2014, 2015). The ice sheet activity in the southwestern Barents Sea initiated at ~2.7 Ma and reached the paleo-shelf at ~1.5 Ma (Knies et al., 2009, 2014; Alexandropoulou et al., 2021). Since then, the southwestern Barents Sea shelf was repeatedly glaciated and further influenced by the Fennoscandian landscape (Andreassen et al., 2007; Laberg et al., 2012). The Pleistocene erosion also provides a reasonable link to the anomalous thermal regimes in the basins as indicated by the present-day well temperatures combined with maturity profiles involved in basin modelling studies (e.g., Cavanagh et al., 2006).

The main structural elements and mega-sequences of the southwestern Barents Sea are seen on the seismic Profile A-A' (Fig. 3, upper panel) and in the summary of the lithostratigraphic and geodynamic events chart (Fig. 2). The NW-SE oriented type-profile, traversing a large part of the southwestern Barents Sea margin shows the main tectonic elements formed in response to the major rift phases (Fig. 2). To the west, the Sørvestsnaget and Bjørnøya basins are characterised by thick Cretaceous sedimentary wedges (Figs. 1 and 3).

2.2.1. Cenozoic uplift and erosion of the region

The present seabed terrain of the southwestern Barents Sea reflects the results of several episodes of Cenozoic uplift and erosion. Different methods have been applied to estimate the timing and to quantify the net erosion in the southwestern Barents Sea (e.g., Henriksen et al., 2011a; Baig et al., 2016; Ktenas et al., 2017, 2019; Lasabuda et al., 2021). Despite having made progress regarding the quantities of the net erosion estimates in the southwestern Barents Sea, there is still a debate on the timing of formation of the erosional products, especially from the Cenozoic period. Due to the hiatus in the rock record, the exact timing of the erosion events and the number of episodes is still poorly constrained. There is strong support by several studies that there is a dominant phase of late Pleistocene exhumation (uplift and erosion) based on perceived mechanisms of erosion attributed to glaciation processes (e.g., Cavanagh et al., 2006; Laberg et al., 2012; Baig et al., 2016; Kishankov et al., 2022). Tectonic uplift is normally linked to the plate reorganization that took place in the Norwegian-Greenland Sea during Eocene and Oligocene times. The glacial contribution to the net erosion took place during the Late Cenozoic isostatic uplift (late Pleistocene). The glacial deposits are separated from the underlying pre-glacial rocks by a prominent reflector, the Upper Regional Unconformity (URU) (e.g., Figs. 3, 4 and 5) (Solheim and Kristoffersen, 1984; Vorren et al., 1991; Laberg et al., 2012). Based on the prominent unconformities in the study area, the Late Cenozoic uplift is considered as an event characterised by two major phases of erosion: one prior to the URU unconformity (pre-glacial) and one after the deposition of the Pleistocene sediments. However, there are basin modelling studies (e.g., Duran et al., 2013a; Baig et al., 2016) that have the main phase of uplift to pre-date the Pleistocene sediments present in the area and a recent study based on U/Th thermochronology that question the significance of the later Pleistocene glacial erosion (Zattin et al., 2016). The latter study indicates that the main phase of uplift started during the Late Miocene-Early Pliocene.

2.2.2. Petroleum systems (and plays) in the southwestern Barents Sea

The Norwegian Petroleum Directorate (NPD) together with the oil industry have identified several petroleum plays, such as the Carboniferous and Lower Permian strata of the Finnmark Platform and Loppa High (Fig. 3; NPD, 2017). The Mesozoic petroleum systems (Triassic, Jurassic and Lower Cretaceous plays) have been described by Doré et al. (2002b). Also there could be Cenozoic source and reservoir rocks in the Sørvestsnaget Basin (Corcoran and Doré, 2002). Petroleum systems in the southwestern Barents Sea consist of various types of source rocks which range from Carboniferous to Cretaceous age (Fig. 2). Some of them have mainly generated gas, while others have most likely generated oil (Ohm et al., 2008; Bjorøy et al., 2010; van Koeverden et al., 2010; Duran et al., 2013b; Killops et al., 2014; Lerch et al., 2016). In particular, five main source rocks are identified, as follows:

1. Gas-prone coal and carbonaceous shales/mudstones from the Lower Carboniferous (the Billefjorden Group). Intercalated shales of the Tettegras Formation coal-bearing sequence may have generated gas and less oil in terms of source rock potential (van Koeverden et al., 2010). This is regarded as being a potential source rock in the area of interest, based on information from analogues on Svalbard and the exploration wells in the southern Barents Sea (e.g., well 7128/4-1, on the Finnmark Platform) (Ohm et al., 2008; van Koeverden et al., 2010; NPD, 2017).

2. Oil-prone carbonaceous mudstones from the Upper Carboniferous-Lower Permian (the Gipsdalen Group) and the Upper Permian marine shales (the Ørret Formation of the Tempelfjorden Group) (Ohm et al., 2008; Killops et al., 2014).

3. Oil- and gas-prone Triassic marine shales (e.g., organic rich Olenekian, Anisian, Ladinian shales, the Sassendalen Group, i.e., the basal Klappmyss, basal Kobbe and basal Snadd

marine shales, which coalesce towards the west as the "Steinkobbe" Formation) (e.g., Bugge and Fanavoll, 1995; Ohm et al., 2008; Abay et al., 2018).

4. The Upper Jurassic black organic-rich shale of the Hekkingen Formation are the principal oil-prone source rocks in the study area and correspond to the hot shales of the Kimmeridge Clay Formation in the North Sea. The Hekkingen Formation is, however, absent or too thin over large parts of the southwestern Barents Sea (Fig. 3) (e.g., Lundschien et al., 2014). Recent petroleum geochemical studies of oil samples revealed the presence of oil derived from source rocks of Jurassic and Triassic age (Duran et al., 2013a,b; Abay et al., 2017; Lerch et al., 2017).

5. Cretaceous source rocks rich in organic material have been identified with potential for forming hydrocarbons (Hagset et al., 2022). While most of the Cretaceous has been eroded in the southwestern Barents Sea, some successions, including the Kolje and Knurr formations, have been preserved in the western deep Cretaceous grabens Harstad, Tromsø and Sørvestsnaget basins (Figs 1 and 2).

Generally, reservoirs are proven in Carboniferous and Permian carbonate and spiculitic deposits and in Triassic, Jurassic and Cretaceous sandstones (Johansen et al., 1993). Only minor discoveries have been made in the Cenozoic sandstones along the margin of the Barents Shelf. The reservoir rocks at the recent Gohta and Alta oil and gas discoveries on the Loppa High consist of Upper Palaeozoic carbonate and siliceous deposits (NPD, 2017). Shales of the Jurassic, Hekkingen and Fuglen formations as well as the Upper Triassic, Snadd and intra Kobbe are usually considered as the principal and most reliable seal in the southwestern Barents Sea. An overview of the most important source and reservoir rocks in the southwestern Barents Sea is shown in Figure 2.

3. Methods and data

In this study, the 2D petroleum system model was generated with PetroMod v2019.1 software package integrating 1D models of selected wells (Fig. 1). The 2D software, forward-simulates the dynamics of basin evolution along a 2D section by deposition and compaction of sediments from the oldest to the youngest event, and additional processes such as hydrocarbon generation, migration, entrapment and losses (Hantschel and Kauerauf, 2009). We thermally calibrated the 1D and 2D models using the EASY%Ro kinetic (Sweeney and Burnham, 1990). Calibration data included vitrinite reflectance and corrected temperature data from exploration wells, as shown in Figure 1. The 1D modelling helped to depict the burial, thermal and maturity history at well locations of the study area while 2D modelling helped to reconstruct oil and gas generation, migration and accumulation along the cross section. Furthermore, representative pseudo-wells were carefully extracted along the 2D section for comparison. Geological information and calibration data (vitrinite reflectance and temperature data) of exploration wells were used. The seismic profile passes through the Bamse (well 7124/3-1), Caurus (7222/11-1 T2) and Johan Castberg (7220/8-1) discoveries (for the exact location, see Fig. 1). Within the vicinity of the seismic profile, a series of wells (e.g., 7128/4-1, 7128/6-1, 7125/4-1, 7125/1-1, 7124/3-1, 7122/2-1 and 7220/7-1) were used to verify and calibrate the 2D model. As it is illustrated in Figure 3, the wells terminate either in the Mesozoic or within the Permian level except for the wells 7128/4-1 and 7128/6-1 that end in the Pre-Devonian basement. Additionally, internal maps of calculated maturity and transformation ratios have been integrated in the study.

The NW-SE oriented type-profile, traversing a large part of the southwestern Barents Sea is used as the model input (Figs. 1 and 3). The Profile A-A' intersects the main tectonic elements such as the Sørvestsnaget Basin, Loppa High, Hammerfest Basin and Finnmark Platform which were formed in response to the major rift phases (e.g., Faleide et al., 1996, 2008). A total of 17

primary horizons from Top Basement to seabed were interpreted and depth converted by Ktenas et al. (2017, 2019), following the high-quality regional velocity model based on seismic processing velocities and check-shots from the public domain and other sources (Meisingset et al., 2018). The structural development is described in Ktenas et al. (2017), integrating uplift, net apparent erosion, heat flow and ice loading (e.g., Nielsen et al., 2013).

3.1.1. Approach to erosion estimation

Several methods for the estimation of net apparent erosion are available, such as, sonic-log and refraction velocity depth trends (e.g., Japsen, 2000; Baig et al., 2016; Ktenas et al., 2017), velocity inversion (Ktenas et al., 2017; 2019), apatite fission track (AFT) analysis (Green and Duddy, 2010), vitrinite reflectance (Gac et al., 2018), mass balance (source-to-sink) calculations (Laberg et al., 2012; Lasabuda et al., 2018) and other methods (Corcoran and Doré, 2005; Anell et al., 2009). Most of these are used as single methods and have their limitations in terms of their applicability and are subject to a certain degree of uncertainty. However, there are integrated studies, which have compared in detail several, completely independent methods, like Ohm et al. (2008) and Baig et al. (2016).

In the basin modelling approach, different methods were utilised to minimise the uncertainty and to integrate their results to establish a consolidated net erosion estimate along the 2D section A-A'. Figure 7 shows conceptual models obtained from different methods, used for the estimation of net apparent erosion (velocity inversion; compaction based net apparent erosion estimates from wells by using sonic logs, regional interpreted profiles and structure grids as well as vitrinite reflectance and temperature data acquired from North Energy database).

Ktenas et al. (2017) developed a velocity inversion Normal Compaction model referred to as the 'Dikte NCT' for use with sonic logs in the southwestern Barents Sea. This model has two baselines: for Cretaceous shale and Lower Jurassic-Upper Triassic sandstone dominated layers. The erosion estimates from the wells are determined by using an alignment of the sonic logs with the 'Dikte NCT' model, (Figure 7a). The 'Dikte NCT' model was then further utilized on regional interpreted seismic profiles and maps depth converted with a check-shot calibrated high-quality regional velocity model (Meisingset et al., 2018; Ktenas et al., 2019). Velocity inversion in interpreted horizons is performed in a set of layers, where mid-point depth and interval velocity are used as inversion inputs. In Figure 7b Layer 1 (green) is a Cretaceous shale (referenced to the Dikte CretShale baseline) and Layer 2 (yellow) is an Upper Triassic sand-shale layer (referenced to the Dikte LJurTrias baseline). The mid-points are plotted together with the baselines in a net apparent erosion window. The estimated erosion is equal to the vertical distance in metres between the points and their respective baselines. The arrows show the uplift path of the points from their maximum depth of burial, when they were located on the baselines, to their present depth (Ktenas et al., 2019).

In general, the vitrinite maturation follows an exponential curve with depth. When plotting the vitrinite reflectance on a logarithmic scale against depth relative to the seabed, a straight line is matched to the data points and the interception of the baseline with the 0.2 %Ro value is measured. In recent sediments deposited at the seabed a value of 0.2 %Ro is assumed. The difference between the maximum depth of burial and the present-day burial depth, at this intercept, represents the net apparent erosion estimate (Fig. 7c).

By integrating the net apparent erosion results from the different methods within the geometric constraint of horizon truncations, an optimised accuracy and areal coverage was achieved. The distribution of the eroded layers was determined by interpreting the depth-

converted truncated horizons within the envelope of the cumulative horizons. Net apparent erosion maps were then included in the model to quality control and remove any inconsistencies. In addition, there was a further subdivision into tectonic and glacigenic events, where the most predominantly erosive event out of these two was explored as an end-member scenario.

3.1.2. Age assignment

The depositional ages are based on information from NPD and available literature (e.g., Larssen et al., 2005; Stemmerik and Worsley, 2005; Cavanagh et al., 2006; Henriksen et al., 2022; NPD, 2022a). The 1D and 2D models also integrate the tectonic uplift and erosion events assigned to events prior of the URU (pre-glacial) and the glacial erosion and uplift events representing the late Pleistocene ice ages. Ice waxing and waning, or in other terms the loading and de-loading of ice, are mimicked by the models (e.g., Cavanagh et al., 2006; Nielsen et al., 2013, 2014, 2015).

3.1.3. Facies assignment

Different petroleum system elements such as source rocks and reservoir rocks are assigned with the respective properties in the 1D and 2D models. The Snadd, Kobbe, Klappmyss and Hekkingen formations are defined as source rocks, the properties of which, such as the initial Hydrogen Index (HI_o), the Total Organic Carbon (TOC_o) and reaction kinetics of the source rocks were assigned to the model (Burnham, 1989). Generally, the initial TOC values for deposits of the Kobbe-Klappmyss, Snadd and Hekkingen formations are typically in the range of about 2-5%, 2-4% and 8-12%, respectively (e.g., Ohm et al., 2008; Abay et al., 2017). The HI_o is approximately 250 mg HC/g TOC, 250 mg HC/g TOC and 350 mg HC/g TOC and the

kerogen types considered are of the Type III and III-II, Type III and III-II, and mixed Type II and III, respectively. We assigned source rocks kinetics from Burnham (1989). Furthermore, the high-amplitude seismic reflectors typical for coal-bearing units of the Carboniferous Tettegras Formation and the uppermost Soldogg Formation (e.g., well 7128/4-1) were assigned as relatively gas-prone coal and coaly source rocks (initial TOC_o 2-8%, HI_o at about 200 mg HC/g TOC, Kerogen Type III and III-II). These occurrences of coal-topped thinning-upward cycles represent deposition on vast flood plains or delta plains (Bugge et al., 1995). In addition, the Ørret Formation of Late Permian age is considered in the models as oil-prone marine shales (initial TOC_o 2-8%, HI_o at about 400 mg HC/g TOC, Kerogen Type III-II and II) although the lateral extent and variation are somewhat less understood. However, the organic rich shales demonstrate their thickest occurrence in the deepest basin and outer ramp areas where dysoxic and anoxic bottom-water conditions prevailed. On the Finnmark Platform and the Loppa High, the shales pass into the shallow-marine deposits of the Røye Formation.

The marginal marine to shallow marine deposits of the Tubåen, Nordmela and Stø formations of Jurassic age were defined as the reservoir rocks, while the Fuglen Formation and the overlying Hekkingen Formation marine shales were defined as the seal rocks. The Tubåen Formation represents predominantly a high-energy marginal marine environment, while the tidal flat to flood plain environments of the Nordmela Formation were followed by a shallow marine environment of the Stø Formation (e.g., Klausen et al., 2017; NPD, 2022a). Sandstones of the Stø Formation are typically moderately to well-sorted and mineralogically mature, where quartz cementation may have reduced the reservoir properties such as porosity (Walderhaug and Bjørkum, 2003). In addition, the marginal to open marine environments, with renewed northwards coastal progradation, characterising deposits of the Triassic Kobbe, Klappmyss, Snadd and Fruholmen formations were assigned as reservoir rocks. Different size of quartz grains and degree of clay coatings on quartz grains were assigned for characterising the chemical

compaction of sandstones of these reservoir facies, based on the Walderhaug Quartz Cementation Model (Walderhaug, 2000a; Walderhaug et al., 2000b; Walderhaug and Bjørkum, 2003).

In addition, reservoir rocks comprise limestones, dolostones and spiculites of the Carboniferous and Permian (e.g., Larssen et al., 2005). Pre-Permian siliciclastic reservoir rocks marked the erosional transition from the basement metasediments into the basal conglomerates and sandstones representative of a braided river system of the Soldogg Formation (Bugge et al., 1995). Overlying deposits characterise alluvial red-bed deposits of the Ugle Formation and the marine deposits of the Falk Formation representing an overall rise in relative sea level in shallow shelf environments.

3.1.4. Boundary conditions

The boundary conditions of the model define the thermal conditions related to the temperature and burial history of the source rocks and consequently the maturation of the organic matter through time. In addition, the reservoir rocks and the influence of temperature on their reservoir properties at various burial depths are integrated. Three main boundary conditions have been defined, the Palaeo-Water Depth (PWD), the Sediment Water Interface Temperature (SWIT) and the Heat Flow (HF).

The PWD trend used in the petroleum systems model was constructed based on the general understanding of the depositional environments (e.g., Larssen et al., 2005; Stemmerik and Worsley, 2005; Smelror et al., 2009; Lerch et al., 2017) as well as from those used for modelling of the adjacent areas in the southwestern Barents Sea (Cavanagh et al., 2006; Duran et al., 2013a). The PWDs vary in time over the entire area by using the de-compaction and

palaeobathymetric approach described by Kjennerud and Sylta (2001). The paleo-surface temperature at sediment-water interface was calculated with the integrated software tool that takes into account the palaeo-water depth and the palaeo-latitude of the study area (Wygrala, 1989).

The paleo-heat flow values in the southwestern Barents Sea vary between 50 and 72 mW/m^2 with an increase towards the west as a result of the lateral heat transfer from the adjacent young ocean (Pascal, 2015). The highest values have been assigned to periods of extensive rifting and faulting, during the Carboniferous, Late Permian-Early Triassic, Late Jurassic-Early Cretaceous and the final rift phase of the Late Cretaceous-Eocene which culminates with continental breakup and seafloor spreading (Fig. 2) (e.g., Cavanagh et al., 2006; Faleide et al., 2008; Clark et al., 2013, 2014; Pascal, 2015). The lowest heat flow values have been assigned to tectonically quite periods. The heat flow trend was created and then assigned to the model from 0 to 345 Ma, with the heat flow ranging between 40 and 70 mW/m^2. During the course of thermal calibration, assignments have been adjusted to better match the well data.

3.1.5. The Golden Zone concept

In recent years, researchers in Norway have developed the concept of the 'Golden Zone' (GZ) for hydrocarbon exploration (e.g., Buller et al., 2005; Nadeau, 2011; Angulo and Vargas, 2022). The GZ refers to a depth range of liquid hydrocarbon window corresponding to temperatures from 60°C to 120°C and thermal maturity of vitrinite reflectance from 0.6% to 1.2% Ro (Bjørkum et al., 2001). Below the GZ (>120°C) occurs the Expulsion Zone (EZ) whilst above the GZ (<60°C) is the Compaction Zone (ComZ), which is also termed the Sealing Zone (SZ) and the Cold Zone (ColZ) (Fig. 8). Bjørkum and Nadeau (1998), Walderhaug (1996) and Nadeau (2011) have documented the impact of clay mineral diagenesis and quartz cementation

on porosity and permeability evolution of the sediments, for sedimentary basins on the Norwegian Continental Shelf and the US Gulf of Mexico Basin. This concept has also been extended to include carbonate reservoirs with a slightly different temperature range for the GZ from 80 to 120°C (e.g., offshore Madagascar) (Bassias and Bertagne, 2015; Roberts and Christoffersen, 2018). However, the definition of the GZ is critical in basins subjected to uplift and erosion such as in the southwestern Barents Sea.

4. Results

4.1. Burial history, erosion and uplift

During the Cenozoic, the southwestern Barents Sea has been affected by several uplift and erosion episodes. This can be clearly illustrated by Figure 3 where thick Cenozoic deposits are observed especially in the Sørvestsnaget Basin and to a lesser extent in the Hammerfest Basin. Towards the Finnmark Platform area, Cenozoic deposition is clearly visible through the prograding Cenozoic sediments that come to down-lap on the Top Cretaceous unconformity (Figs. 4, 5 and 6). Furthermore, such areas in the southwestern Barents Sea tend to be exposed to lower temperatures, which can have a large impact on the maturity of the source rocks.

Several episodes of tectonic events have affected the area since the Caledonian Orogeny in the early Devonian times. The Caledonian event was accompanied by sedimentary deposition across the southwestern Barents Sea, as it is illustrated by the Early Devonian deposition interpreted in Figure 3. Mid Carboniferous and Permian rifting events were followed by regional subsidence during the Triassic to Early Jurassic times. The Jurassic and Early Cretaceous subsidence is clearly marked in the Sørvestsnaget Basin, as it allowed for Cretaceous and

Cenozoic deposition to occur and fill the basin creating a depocenter towards the west, as can be observed in Profile A-A' (Fig. 3).

The deposition and erosion of the layers at different time steps is shown in Figure 9. This geological development at different time periods has been obtained by using the back-stripping technique. Back-stripping is a basin analysis approach that is used to quantitatively estimate the depth that the basement would be in the absence of sediment and water loading. Furthermore, in the study area, by progressively removing each stratigraphic sequence and decompacting sediments, it was possible to restore horizons to estimated water depths at different time periods (e.g., Kjennerud and Sylta, 2001). In addition, the geological structure of the basins and their major faults, featuring the predominant geological structure of the Loppa High, are dated back to the beginning of the Early Jurassic. The Late Cretaceous-Cenozoic sediments are overlying unconformably the highly faulted Triassic and older sediments.

The most important geological events that were used as model input in post-Caledonian times include the following:

- A Devonian and Early Carboniferous rifting phase, predominantly fluvial and alluvial sediments and coal deposits
- Middle Carboniferous to mid-Permian quiet tectonic phases, with deposition of platform carbonates and thick basinal evaporites
- A Late Permian to Early Triassic rifting phase. A cooler climate and siliciclastic input, associated to a marine environment
- Triassic represented by large-scale clinoforms prograding in a northwestern direction
- A lower-Middle Jurassic period which was relatively quiet when the main reservoirs of the Realgrunnen Sub-Group (Stø, Nordmela, Tubåen and Fruholmen formations) were deposited

- An Upper Jurassic to Lower Cretaceous rifting phase
- Cenozoic and tectonic events (e.g., North Atlantic Ocean spreading) with associated uplift and erosion
- Quaternary events influenced by ice ages together with associated erosion and uplift.

4.2. Source rock maturity

An independent maturity map of the Hekkingen Formation source rock based on the maximum depth of burial at the Base Cretaceous Unconformity (BCU) level, has been produced illustrating the regional differences in the southwestern Barents Sea (Fig. 10). The maximum depth of burial has been calculated by applying a regional erosion estimate map from Ktenas et al. (2017) and Ktenas et al. (2019). The equation applied here is as follows: 'Maximum depth of burial' = ('Present depth below MSL' – 'Water depth') + 'Net apparent erosion'. The maturation map is most likely a qualitative approach where the average geothermal gradient has been calculated from wells (e.g., Henriksen et al., 2021).

Large areas are at an immature stage in the eastern part of the study area. Towards the west, in the Sørvestsnaget Basin, in some parts of Tromsø and Bjørnøya basins this source rock was gas-mature to over-mature at the time of maximum burial, implying that the oil generation started before the time of maximum burial. Only narrow zones along the eastern part of Bjørnøya, Sørvestsnaget, Tromsø basins generated oil at that stage, in addition to minor areas in the Hammerfest Basin and the southwestern part of the Nordkapp Basin.

To investigate the depth of the oil and gas windows, it was also necessary to apply vitrinite reflectance and temperature data in constructed 1D models of selected wells along the 2D model. Generally, the thermal maturity at which the onset of oil generation takes place is

correlated with a reflectance of about 0.5-0.6%Ro and the level at which there is enough efficient oil generation able to onset the expulsion of hydrocarbons is at about 0.65 to 0.7%Ro (e.g., Sweeny and Burnham, 1990). They are both strongly related to the reaction kinetics of the source rock; however, the ability of the source rock to expel hydrocarbons is also dependent on rock properties. Typically, the termination of oil generation takes place with vitrinite reflectance of about 0.85-1.35%Ro, and the onset of the wet and dry gas windows is from 1.35-2.0%Ro (e.g., Tissot and Welte, 1984; Sweeny and Burnham, 1990; Magoon and Dow, 1994; Welte et al., 2012). However, these oil and gas windows vary among source rocks with different kinetics.

The modelling results, as illustrated in Figure 11a, show source rocks maturity along the 2D profile expressed as vitrinite reflectance. All of the source rocks in the Sørvestsnaget Basin are mainly exhausted and overmature, whereas in the Loppa High area they are mature and range from oil to dry gas (Fig. 11a). Over the Loppa High, the oldest source rocks are dry gas mature, whereas those lying immediately above are wet gas mature on the steep western flank of the Loppa High and in the oil window on the eastern flank, which become wet gas mature as we move further eastwards. Generally, the youngest source rocks are early oil mature on both flanks of the Loppa High. Further east in the study area, the older source rocks tend to be overmature or dry gas mature and towards the Finnmark Platform, their maturity ranges from dry gas to wet gas to reach the late oil window as we go from west to east. The younger source rocks pass also from dry gas to wet gas to predominantly the oil window and even to immature (Jurassic) and marginal mature (Triassic). This transition begins further and further westwards the younger the source rocks are.

4.2.1. Hydrocarbon generation history

The transformation ratio represents an indicator of hydrocarbon generation of the source rock units based on the assigned reaction kinetics (e.g., Burnham, 1989). In Figure 11b, the progressing maturity of the source rocks is illustrated for the present day in terms of a transformation ratio expressed as a percentage of kerogen to petroleum conversion. The youngest source rocks (Jurassic), for example, in the Hammerfest Basin and the Finnmark Platform, range from up to 75% in the Hammerfest Basin to roughly 25% in the Nysleppen Fault Complex (Fig. 11b). On the Finnmark Platform, the transformation ratio decreases updip from roughly 25% to near 0% and remains at very low ratios. This indicates the presence of immature and marginal mature source rocks for most of the extent of the Finnmark Platform.

Figure 11c shows the critical moment corresponding to the time of the highest probability of entrapment and preservation of hydrocarbons. In the 2D model the 'critical moment' is defined as the moment when transformation ratio reached 50% (i.e., 50 % of the labile kerogen within the source rock has been converted to petroleum). For a successful charge this should happen after trap formation with a proper seal (Magoon and Dow, 1994). The source rocks considered here include the Tettegras, Ørret, Kobbe-Klappmyss and Hekkingen formations. The most common critical moment over the study area ranges from the mid Cretaceous to older ages for most source rocks, especially for the oldest ones, throughout the study area. A more recent critical moment is in general observed for the younger source rocks in the eastern part of the 2D profile and on the eastern flank of the Loppa High. The youngest source rocks in the Hammerfest Basin are characterised by a transition of the critical moment from the Late Cretaceous in the west to near present day in the east. Furthermore, the more recent critical moment is also encountered, on the Nysleppen Fault Complex (close to the 7124/3-1, 7125/1-1 and 7125/4-1 wells) as well as in the eastern part of the study area, on the Finnmark Platform (close to the 7128/4-1 and 7128/6-1 wells) where it is close to the present day.

A close-up of the eastern part of the study area is shown in Figure 12, including the eastern part of the Hammerfest Basin, the Nysleppen Fault Complex area and the Finnmark Platform. The hydrocarbon zonation shown in Figure 12 is dependent on source rock kinetics and their burial history. In Figure 12a is shown the source rock kerogen Type II (organofacies B *sensu* Pepper and Corvi, 1995), which is typically of the organic rich marine shales of the Upper Jurassic Hekkingen Formation and the Upper Permian source rock. In Figure 12b, kerogen Type IIIH (organofacies DE) is used, which characterises a more humic coaly source rock, which is relatively gas prone with some oil potential. The illustrations of kerogens of Type II (B) and of Type IIIH (DE) in Figure 12 show the oil and gas generation and the present-day maturity of the source rocks in terms of immature, oil, gas and overmature zones. Generally, the kerogen types show similar trends along the 2D profile. However, the depths of the hydrocarbon zonation reflect, as expected, the reactivity of the different kinetics of the oil-prone versus the gas-prone source rocks. The older and therefore deeper buried source rocks are described as overmature in the study area (Fig. 12). In the Nysleppen Fault Complex area in the west, the Pre-Permian source rock Tettegras is overmature whereas the younger Permian source rock is overmature in the western part of the fault complex and reaches the gas zone in the eastern part. The Kobbe-Klappmyss source rock shows a transition from overmature, gas to oil zone in the western part of the fault complex, whereas in the eastern part the source rock reaches the oil zone.

As we move to the east, in the Finnmark Platform area, the Pre-Permian source rock continually transits from the oil to the gas zone (Fig. 12). In the same area, as we move upwards in geological time we pass into the more oil-prone Permian source rocks in the oil zone. In this eastern part, the even younger source rocks (Kobbe-Klappmyss and Hekkingen formations) are mainly described as immature rocks.

In Figure 12c, the expulsion onset, expressed in million years, is illustrated as a close-up of the eastern part of the 2D profile, similar to Figures 11a and 11b. Expulsion onset corresponds to the timing of when the different source rocks are predicted to begin to expel oil and gas into the adjacent rocks; i.e., the onset of secondary migration out of the source rock. In the eastern part of the Hammerfest Basin and Nysleppen Fault Complex areas, the Pre-Permian source rocks are characterised by expulsion onset prior to the Mid Cretaceous. The Permian source rocks are also described by a similarly early expulsion onset age in the western part of the close-up 2D profile (Fig. 12c), but which is significantly postponed to about 40-100 Ma updip of the Finnmark Platform. The age of the onset of expulsion from the Kobbe-Klappmyss source rock is gradually later from west to east from about 100 Ma to near 0 Ma. Overall, the shallow burial depth of the oil-prone Hekkingen shales results in the youngest expulsion onset seen for the study area, roughly equivalent to the mid Cenozoic or later.

The 2D profile in Figure 13 illustrates the transformation ratio of the different source rocks at present day and the three locations of time extractions for vitrinite reflectance of the source rocks. Pre-Permian Tettegras, Permian Ørret, Triassic Kobbe-Klappmyss and Upper Jurassic Hekkingen, are treated as occurring throughout the 2D profile. Generally, less mature source rocks are observed updip and on the Finnmark Platform compared with the basin areas to the west. On the Finnmark Platform, the Triassic and Jurassic source rocks are immature, implying that any hydrocarbons found need to be derived from the older source rocks on the platform or need to be generated in deeper settings off the platform.

4.2.2 Reservoirs

Reservoir rocks play an important role when assessing the petroleum system as well as the related prospectivity in an area. The presence of reservoir rocks is normally de-risked by

depositional models, whereas the quality of reservoir rocks is related to depositional mechanisms such as sorting of grains (mechanical compaction) and the diagenetic processes influenced by temperature variation (chemical compaction) through the burial history. Variations in the present-day temperature and the predicted maximum temperature along the 2D profile are shown in Figure 14a and 14b, respectively. This illustrates the differences between the past and the present-day temperatures before and after the uplift-erosion events (see also Figure 8). Special attention should be paid on the scale of temperatures reflecting biodegradation (Fig. 14b). Below approximately 60-80°C there are larger chances of finding biodegraded oil (e.g., Wilhelms at al., 2001; Wenger et al., 2002; Justwan et al., 2006). The elevated temperatures that have been experienced in the past are translated into palaeo-pasteurisation and consequently sterilisation of the reservoir in the past.

The predicted effective porosity of reservoir rocks is shown in Figure 15. The effective porosity is dependent on the mechanical compaction and rock properties such as chemical compaction incorporating quartz content, quartz grain coatings and grain size for the modelling of quartz cementation. In general, the effective porosity increases from west to east along the 2D profile and similarly in the reservoir rocks which are of younger age and found at shallower burial depths. The effective porosity varies from about 5% to more than 15-20%, a value which is encountered on the Finnmark Platform (Fig. 15).

Chemical compaction and the associated loss of porosity is shown in Figure 16. The chemical compaction of sandstones resulting from quartz cementation can be controlled by the amount of clay coatings on quartz grains as a function of grain size and the temperatures that the reservoir rock has experienced through time. The quartz cementation modelling was carried out for sandstones of Palaeozoic, Triassic and Jurassic age (Fig. 16).

Overall, the chemical compaction of the Triassic and Jurassic sandstones reaches up to about 15% porosity reduction with the highest degree of cementation in the basin areas being found in the west whilst the smallest reduction of effective porosity is found in the Finnmark Platform area. Therefore, the influence of diagenetic processes on the reservoir quality is here reflecting the degree of quartz cementation and its relation with maximum temperature (pre-erosion) through burial history, where any uplift-erosion events would then reduce the temperature and the rate of cementation. The cementation and its porosity loss are dependent on the degree of clay coatings on quartz grain sizes (typically reflecting the depositional environment) as well as temperature and burial history.

5. Discussion

5.1. The Golden Zone in the southwestern Barents Sea

The temperature gradients for the reservoirs vary from place to place and thus, the GZ is expected to be found at somewhat different depths. On the Norwegian Continental Shelf, the depth of the GZ is ranging from two to around four kilometres (base of the GZ, 120°C) while in some areas it can be found between one to two kilometres. Based on the maximum burial depth of several discoveries (e.g., Wisting, Hanssen, Alta, Skrugard, Gohta, Snøhvit and Havis), the base of the Golden Zone has been shifted from about 3.7 km to 2.5 km depth (e.g., Nadeau, 2016).

These discoveries have been investigated by focusing on some key events, which have implications with respect to the GZ concept in the southwestern Barents Sea. The key element considered is the thermal regime of the area in order to use the estimates from the wells along

the 2D profile. Nearby wells are also used since the E-W section (Fig. 3) covers a number of different tectonic domains and these are expected to show considerable variation over the region.

An example of the application of the GZ concept for the southwestern Barents Sea is illustrated in Figure 17. Here we observe how temperature data from the Drill Stem Test (DST) and the Bottom Hole temperatures (BHT) increase relatively linearly with an increase in depth. This increase in the temperature trend also corresponds to the passing from the Compaction Zone (Sealing Zone) to the GZ and finally to the Expulsion Zone. An interesting observation is that different estimates of the magnitude of uplift and erosion ((based on vitrinite reflectance data and estimates from Ktenas et al. (2017, 2019)) all indicate a significant shift in depth and associated maximum temperature to the lower present-day temperatures measured by DST and BHT.

Furthermore, the glacigenic erosion and later uplift events introduced a low temperature at the base of the ice, resulting in a less steep temperature gradient and thereby a cooling of the succession (Cavanagh et al., 2006; Nielsen et al., 2013, 2014). As such, the southwestern Barents Sea was subjected to an accelerating temperature change by both tectonics and ice dynamics during the late Cenozoic, expressed by the large change in temperatures from the time of maximum burial depth (typically maximum temperature) and the temperatures measured at the present day (Figs. 14a, b and 17).

5.2. Petroleum systems

The petroleum systems have been studied in more detail along the 2D profile in the Finnmark Platform, southwestern Nordkapp Basin and the Nysleppen Fault Complex area. Several discoveries have been made in the Norwegian sector of the Barents Sea east of 26 ºE

(Figs. 1 and 10) including three deeply penetrating exploration wells 7128/4-1, 7128/6-1 and 7130/4-1. Well results are here interpreted in the light of our basin models focusing on the Finnmark Platform area.

The discovery well 7128/4-1 is located on the Finnmark Platform and is classified as an oil and gas discovery in Upper Permian spiculites (Røye Formation) within the Tempelfjorden Group (NPD, 2022a). The Upper Permian spiculite play is proven and the reservoir presence and quality have been demonstrated in the 7128/4-1 well. In particular, the oil found in the Røye Formation on the Finnmark Platform is distinctly different from other oils (e.g., oils in the Kobbe and Klappmyss formations in the Goliat field) and characterised by heavy carbon isotopes (e.g., Lerch et al., 2016). This strongly indicates the presence of a Palaeozoic source rock despite the find of a small volume. The oil could have been either sourced from the coal-bearing Tettegras Formation of Carboniferous age or from the Permian Ørret as an alternative candidate (van Koeverden et al., 2010; Henriksen et al., 2022). Coal-bearing sections of similar age have been identified on Svalbard and Bjørnøya suggesting that coal distribution extends over large areas in the southwestern Barents Sea, with a lesser extent towards the graben features (Larssen et al., 2005). Reservoir rocks have also been recognised in dolomitised carbonates, which are encountered in the Ørn Formation (late Carboniferous-early Permian) in well 7128/6-1 where minor oil shows are also recorded. Visean sandstones (Billefjorden Group) encountered in both wells exhibit highly variable reservoir qualities and this represents an important risk issue in these plays.

Our 2D model predicts that the Permian source rocks are within the oil window and the even younger source rocks of the Kobbe, Klappmyss and Hekkingen formations are mainly immature to marginal mature source rocks (Figs. 11a and 12). As can be seen from the interpreted regional profiles (e.g., Fig. 6), the Finnmark Platform has undergone a major uplift.

Based on sonic velocity measurements (Ktenas et al., 2017) the net apparent erosion for the wells 7128/4-1 and 7128/6-1 is at about 1450 and 1500 metres, respectively, which is consistent with previous studies (e.g., Henriksen et al, 2011). There, the net erosion estimates have been assessed from the lower part of the Triassic section. Similar estimates have been obtained in stratigraphic layers (Cretaceous and Triassic) in the eastern part of the Finnmark Platform (Profile A-A') as well as in structure maps based on the velocity inversion analysis (Ktenas et al., 2019). The difference in present day temperature and the maximum temperature before and after the uplift and erosion events indicate alteration of the reservoir quality due to the diagenetic processes (Fig. 14). In particular, the effective porosity of the Pre-Permian siliciclastic deposits in the Finnmark Platform appears to be less affected through the temperature and burial history towards the eastern Norwegian Barents Sea (Fig. 15).

Indications of secondary porosity in carbonates with similar processes have been observed in the Gohta discovery in the Loppa High (Brunstad and Rønnevik, 2023). These indications increase the potential of the reservoir rocks of the Permian. Following the evolution that took place later in the Triassic, a large delta begun to fill up the Barents Sea with clastic sediments. The existence of a 'mountain range' (Uralides from Palaeozoic) was considered as the main provenance area, thus providing an explanation of the aforementioned event. Large scaled clinoforms and fluvial deposits in the Finnmark Platform have also been observed throughout the southwestern Barents Sea. The Triassic interval has the potential for containing petroleum reservoir rocks (Glørstad-Clark et al., 2011; Eide et al., 2018; Henriksen et al., 2022).

Recently, the primary exploration target for the well 7130/4-1 (Ørnen prospect), which is located east of our study area on the Finnmark Platform, was to prove petroleum in carbonate and spiculite deposits of the Røye Formation (NPD, 2022a). The secondary exploration target aimed to prove petroleum in underlying carbonates and sandstones of the Ørn and Soldogg

formations of Carboniferous and Permian ages. In the primary exploration target, well 7130/4-1 encountered an approx. 40-metre thick spiculite reservoir in the Røye Formation but was characterised by a poor reservoir quality and traces of oil. In the secondary exploration target, the well proved minor shows of petroleum in the Ørn Formation. In this well, the formation is about 180 metres thick but is mainly tight. A gas column height of 5 m was encountered in sandstones with moderate reservoir quality of the Soldogg Formation (NPD, 2022a). Furthermore, a recent gas discovery was confirmed in the Finnmark Platform, namely the 7122/9-1 (Lupa) well in Lower Triassic Havert Formation (NPD, 2022a). Such findings continue to maintain the Finnmark Platform's status as a region of considerable interest for further exploration.

5.3. Uncertainty in data and modelling

The uncertainty is often related to the basin geometry since it relies on uncertain seismic interpretation and depth of the stratigraphic horizons based on a regional velocity model (e.g., Baur et al., 2010). Additional uncertainty in the modelling is related to thermal boundary conditions (e.g., paleo-heat flow) and geochemical properties of source rocks and their kinetics. Some uncertainty is also related to the estimation of the magnitude and timing of uplift and erosion events (e.g., Ktenas et al., 2017, 2019 and references therein).

6. Conclusions

The aim of this study was to evaluate the impact of maximum burial and net apparent erosion to the petroleum systems in the southwestern Barents Sea. This is illustrated by mapping and modelling a regional 2D profile through the southwestern Barents Sea. The estimates of net apparent erosion along the 2D profile were also integrated from vitrinite reflectance, temperature

as well as by velocity inversion of sonic logs, profiles, and maps. The uplift-erosion events were subdivided into tectonic and glacigenic events and the most predominant erosion event out of these two was investigated as end-member scenarios.

The selected end-member of the uplift-erosion scenario determines for what length of time the source rock is retained at great depth and therefore the time it takes for generating and expelling oil and gas from the deeper kitchen area, until the source rock is uplifted into the low temperature regime. Time-wise this could in principle also control how effective expulsion from the source rock is; i.e., assuming that the longer the time of exposure to higher temperatures and pressures is, the greater the possibility of larger amounts being expelled from the source rock.

Deep burial depth and exposure to higher temperatures prior to uplift and erosion, clearly influences the reservoir quality and can be used directly as a prediction tool in the evaluation of the reservoir quality regionally. At several places, the porosity is varying due to mechanical compaction and the temperature-controlled diagenesis resulting in lower porosity than expected at certain depths compared to other basins not subjected to severe uplift and erosion.

An understanding of maturity history at various well locations was achieved by carrying out 1D modelling for a selected number of wells in the region. The Barents Sea is complex, but even the simplest basin setup with multiple source rocks shows different timing for hydrocarbon generation; i.e., emphasizing the real complexities such as regional tilting, multiple sub-basins, different erosion events, ice ages, net erosion/uplift. This study has demonstrated that the expulsion may have taken place since Triassic and up to late Tertiary times. It is expected that the hydrocarbon expulsion ceased during the late uplift periods. A predicted maturity map reflecting the oil and gas windows for the most prominent source rock, the Hekkingen Formation, clearly indicates that large areas towards the east have most likely never reached the oil window. In the deep basins towards the west, the Hekkingen Formation has reached the oil and gas window at maximum burial and the deeper source rocks are now overmature.

Simulation results in the 2D modelling showed that the Upper Jurassic source rock is immature to marginal mature over large parts of the eastern part of the study area. The expectations of future discoveries in the area are high, especially for those areas and depths which are characterised by high chargeability of traps associated with the pre-Jurassic source kitchens and the porous reservoir rocks. Locally, however, prospectivity varies considerably within the region. The highest potential for oil is expected in the western areas, while gas and gas-condensate from pre-Jurassic source kitchens will be dominant in most of the eastern areas of the Norwegian Barents Sea.

Accordingly, the strategy for hydrocarbon exploration in severely exhumed basins has to be aligned with the magnitude and timing of the uplift and erosion events such as in the Barents Sea, exploring at shallower depths than previously.

Acknowledgements

Funding has been received from the People Programme (Marie Curie Actions) of the European Union's Seventh Framework Programme FP7/2007-2013/ under REA grant agreement No 317217. The research forms part of the GLANAM (GLAciated North Atlantic Margins), www.glanam.org Initial Training Network. This also corresponds to a contribution to the RCN-funded project "Research Centre for Arctic Petroleum Exploration" (ARCEx) (grant 228107). We sincerely acknowledge the Section Editor Tiago Alves, Balazs Badics, Domenico Chiarella and Rüdiger Lutz for the thorough review and constructive feedback during the review process. Thanks to Searcher Seismic and TGS ASA for being allowed to publish the seismic data. Special acknowledgments go to North Energy ASA for providing access to Schlumberger (SLB) Petrel and PetroMod software as well as to in-house materials.

References

Abay, T.B., Karlsen, D.A., Pedersen, J.H., Olaussen, S., Backer-Owe, K., 2018. Thermal maturity, hydrocarbon potential and kerogen type of some Triassic–Lower Cretaceous sediments from the SW Barents Sea and Svalbard. Petroleum Geoscience 24(3), 349–373. https://doi.org/10.1144/petgeo2017-035.

Andreassen, K., Odegaard, C.M., Rafaelsen, B., 2007. Imprints of former ice streams imaged and interpreted using industry three-dimensional seismic data from the south-western Barents Sea. In: Davies, R.J., Posamentier, H.W., Wood, L.J., Cartwright, J.A. (Eds.), Seismic Geomorphology: Applications to Hydrocarbon Exploration and Production. Geological Society, London, pp. 151–169. Special Publications 277. https://doi.org/10.1144/GSL.SP.2007.277.01.09.

Alexandropoulou, N., Winsborrow, M., Andreassen, K., Plaza-Faverola, A., Dessandier, P.A., Mattingsdal, R., Baeten N., Knies, J., 2021. A Continuous Seismostratigraphic Framework for the Western Svalbard-Barents Sea Margin Over the Last 2.7 Ma: Implications for the Late Cenozoic Glacial History of the Svalbard-Barents Sea Ice Sheet. Frontiers in Earth Science, 9, 327. https://doi.org/10.3389/feart.2021.656732.

Amantov, A., Fjeldskaar, W., 2018. Meso-Cenozoic exhumation and relevant isostatic process: The Barents and Kara shelves. Journal of Geodynamics 118, pp. 118–139. https://doi.org/10.1016/j.jog.2017.12.001.

Anell, I.A.M., Thybo, H., Artemieva, I., 2009. Cenozoic uplift and subsidence in the North Atlantic region: geological evidence revisited. Tectonophysics 474, 78–105. https://doi.org/10.1016/j.tecto.2009.04.006.

Angulo, A., Vargas, C.A., 2022. Global distribution of the hydrocarbon Golden Zone. Marine and Petroleum Geology, 144, 105832. https://doi.org/10.1016/j.marpetgeo.2022.105832.

Baig, I., Faleide, J.I., Jahren, J., Mondol, N.H., 2016. Cenozoic exhumation on the southwestern Barents Shelf: Estimates and uncertainties constrained from compaction and thermal maturity analyses. Marine and Petroleum Geology 73, 105–130. https://doi.org/10.1016/j.marpetgeo.2016.02.024.

Baur, F., Littke, R., Wielens, H., Lampe, C., Fuchs T., 2010. Basin modeling meets rift Analysis-a numerical modeling study from the Jeanne d'Arc basin, offshore Newfoundland, Canada. Marine and Petroleum Geology 27, 585–599. https://doi.org/10.1016/j.marpetgeo.2009.06.003.

Bassias, Y., Bertagne, R., 2015. Study updates uplift-erosion correlation, Davie fracture zone. Oil & Gas Journal, 113 (9), 64–75.

Bellwald, B., Waage, M., Planke, S., Lebedeva-Ivanova, N., Polteau, S., Tasianas, A., Bünz, S., Plaza-Faverola, A.A., Berndt, C., Stokke, H.H., Millett, J., Myklebust, R., 2018a. Monitoring of CO_2 leakage using high-resolution 3D seismic data – Examples from Snøhvit, Vestnesa Ridge and the Western Barents Sea. 5th CO_2 Geological Storage Workshop, EAGE Extended Abstracts 2018. https://doi.org/10.3997/2214-4609.201802965.

Bellwald, B., Planke, S., Piasecka, E.D., Matar, M.A., Andreassen, K., 2018b. Ice-stream dynamics of the SW Barents Sea revealed by high-resolution 3D seismic imaging of glacial deposits in the Hoop area. Marine Geology 402, 165–183. https://doi.org/10.1016/j.margeo.2018.03.002.

Bjorøy, M., Hall, P.B., Ferriday, I.L., Mørk, A., 2010. Triassic Source Rocks of the Barents Sea and Svalbard. AAPG Search and Discovery Article #10219, 2009.

Bjørkum, P.A., Nadeau, P.H., 1998. Temperature controlled porosity/permeability reduction, fluid migration, and petroleum exploration in sedimentary basins. Australian Petroleum Production and Exploration Association Journal 38, 453–464. https://doi.org/10.1071/AJ97022.

Brunstad, H., Rønnevik, H.C., 2023. Loppa High Composite Tectono-Sedimentary Element, Barents Sea. Geological Society, London, Memoirs, 57(1), M57-2020. https://doi.org/10.1144/M57-2020-3.

Bugge, T., Fanavoll, S., 1995. The Svalis Dome, Barents Sea – a geological playground for shallow stratigraphic drilling. First Break 13, 237-251. https://doi.org/10.3997/1365-2397.1995012.

Bugge, T., Mangerud, G., Elvebakk, G., Mørk, A., Nilsson, I., Fanavoll, S., Vigran, J.O., 1995. The Upper Palaeozoic succession on the Finnmark Platform, Barents Sea. Norsk Geologisk Tidsskrift 75, 3–30.

Buller, A.T., Bjørkum, P.A., Nadeau, P.H., Walderhaug, O., 2005. Distribution of Hydrocarbons in Sedimentary Basins. Research & Technology Memoir No. 7, Statoil ASA, Stavanger, 15 pp.

Burnham, A.K., 1989. A simple kinetic model of petroleum formation and cracking (Technical Report No. UCID-21665). Lawrence Livermore National Lab., CA (USA).

Cavanagh A.J., di Primio R., Scheck-Wenderoth M., Horsfield B., 2006. Severity and timing of Cenozoic exhumation in the southwestern Barents Sea. Journal of Geological Society, 163, 761–774. https://doi.org/10.1144/0016-76492005-146.

Clark, S.A., Faleide, J.I., Hauser, J., Ritzmann, O., Mjelde, R., Ebbing, J., Thybo, H., Flüh, E., 2013. Stochastic velocity inversion of seismic reflection/refraction travel time data for rift

structure of the southwest Barents Sea. Tectonophysics 593, 135–150. https://doi.org/10.1016/j.tecto.2013.02.033.

Clark, S.A., Glørstad-Clark, E., Faleide, J.I., Schmid, D., Hartz, E.H., Fjeldskaar, W., 2014. Southwest Barents Sea rift basin evolution: comparing results from back-stripping and time-forward modelling. Basin Research 26, 550–566. https://doi.org/10.1111/bre.12039.

Corcoran, D.V., Doré, A.G., 2002. Top seal assessment in exhumed basin settings - some insights from the Atlantic Margin and borderland basins. In: Koestler, A.G. and Hunsdale, R. (Eds.) Hydrocarbon Seal Quantification. NPF (Norwegian Petroleum Society) Special Publication 11, Elsevier, Amsterdam, 89–107. https://doi.org/10.1016/S0928-8937(02)80009-1.

Dimakis, P., Braathen, B.I., Faleide, J.I., Elverhøi, A., Gudlaugsson, S.T., 1998. Cenozoic erosion and the preglacial uplift of the Svalbard-Barents Sea region. Tectonophysics 300, 311–327. https://doi.org/10.1016/S0040-1951(98)00245-5.

Doré, A.G., Jensen, L.N., 1996. The impact of late Cenozoic uplift and erosion on hydrocarbon exploration: offshore Norway and some other uplifted basins. Global Planetary Change 12, 415–436. https://doi.org/10.1016/0921-8181(95)00031-3.

Doré, A.G., 1991. The structural foundation and evolution of Mesozoic seaways between Europe and the Arctic. Palaeogeography, Palaeoclimatology, Palaeoecology 87(1-4), 441–492. https://doi.org/10.1016/0031-0182(91)90144-G.

Doré, A.G., Cartwright, J.A., Stoker, M.S., Turner, J.P. and White, N., 2002a. Exhumation of the North Atlantic margin: introduction and background. In: Doré, A.G., Cartwright, J.A., Stoker, M.S., Turner, J.P., White, N. (Eds.), Exhumation of the North Atlantic Margin: Timing, Mechanisms and Implications for Petroleum Exploration, vol. 196. Geological

Society London, Special Publications, pp. 1–12. https://doi.org/10.1144/GSL.SP.2002.196.01.01.

Doré, A.G., Corcoran, D.V., Scotchman, I.C., 2002b. Prediction of the hydrocarbon system in exhumed basins, and application to the NW European margin. In: Doré, A.G., Cartwright, J.A., Stoker, M.S., Turner, J.P., White, N. (Eds.), Exhumation of the North Atlantic Margin: Timing, Mechanisms and Implications for Petroleum Exploration, vol. 196. Geological Society London, Special Publications, pp. 401–429. https://doi.org/10.1144/GSL.SP.2002.196.01.21.

Doré, A.G., Dahlgren, T., Flowerdew, M.J., Forthun, T., Hansen, J.O., Henriksen, L.B., Kåsli, K., Rafaelsen, B., Ryseth, A.E., Rønning, K., Similox-Tohon, D., Stoupakova, A., Thießen, O., 2023. South-Central Barents Sea Composite Tectono-Sedimentary Element. Geological Society, London, Memoirs, 57(1), M57-2017. https://doi.org/10.1144/M57-2017-42.

Duran, E.R., di Primio, R., Anka, Z., Stoddart, D., Horsfield, B., 2013a. 3D-basin modelling of the Hammerfest Basin (southwestern Barents Sea): a quantitative assessment of petroleum generation, migration and leakage. Marine and Petroleum Geology 45, 281–303. https://doi.org/10.1016/j.marpetgeo.2013.04.023.

Duran, E.R., di Primio, R., Anka, Z., Stoddart, D., Horsfield, B., 2013b. Petroleum system analysis of the Hammerfest Basin (southwestern Barents Sea): comparison of basin modelling and geochemical data. Organic Geochemistry 63, 105–121. https://doi.org/10.1016/j.orggeochem.2013.07.011.

Eide, C.H., Klausen, T.G., Katkov, D., Suslova, A.A., Helland-Hansen, W., 2018. Linking an Early Triassic delta to antecedent topography: Source-to-sink study of the southwestern Barents Sea margin. GSA Bulletin, 130(1-2), 263-283. https://doi.org/10.1130/B31639.1.

Faleide, J.I., Solheim, A., Fiedler, A., Hjelstuen, B.O., Andersen, E.S., Vanneste, K., 1996. Late Cenozoic evolution of the western Barents Sea-Svalbard continental margin. Global Planetary Change 12, 53–74. https://doi.org/10.1016/0921-8181(95)00012-7.

Faleide, J.I., Tsikalas, F., Breivik, A.J., Mjelde, R., Ritzmann, O., Engen, O., Wilson, J., Eldholm, O., 2008. Structure and evolution of the continental margin off Norway and Barents Sea. Episodes 31, 82–91. https://doi.org/10.18814/epiiugs/2008/v31i1/012.

Gac, S., Hansford, P.A., Faleide, J.I., 2018. Basin modelling of the SW Barents Sea. Marine and Petroleum Geology, 95, 167-187. https://doi.org/10.1016/j.marpetgeo.2018.04.022.

Gasser, D., 2014. The Caledonides of Greenland, Svalbard and other Arctic areas: Status of research and open questions. In: New Perspectives on the Caledonides of Scandinavia and Related Areas, Geological Society Special Publications, vol. 390, edited by F. Corfu, D. Gasser., D.M. Chew, pp. 93–129, Geological Society, London. https://doi.org/10.1144/SP390.17.

Gernigon, L., Brönner, M., Roberts, D., Olesen, O., Nasuti, A., Yamasaki, T., 2014. Crustal and basin evolution of the southwestern Barents Sea: from Caledonian orogeny to continental breakup. Tectonics, 33(4), 347–373. https://doi.org/10.1002/2013TC003439.

Glørstad-Clark, E., Birkeland, E.P., Nystuen, J.P., Faleide, J.I., Midtkandal, I., 2011. Triassic platform-margin deltas in the western Barents Sea. Marine and Petroleum Geology, 28(7), 1294-1314. https://doi.org/10.1002/2013TC003439.

Green, P.F., Duddy, I.R., 2010. Synchronous Exhumation Events Around the Arctic Including Examples from Barents Sea and Alaska North Slope. In: Petroleum Geology Conference Series, vol. **7**. Geological Society, London, pp. 633–644. https://doi.org/10.1144/0070633.

Hagset, A., Grundvåg, S.A., Badics, B., Davies, R., Rotevatn, A., 2022. Tracing Lower Cretaceous organic-rich units across the SW Barents Shelf. Marine and Petroleum Geology, 140, 105664. https://doi.org/10.1016/j.marpetgeo.2022.105664.Hartz, E.H., Medvedev, S., Schmid, D., Faleide, J.I., Iyer, K., Scheirer, A. H., Hartwig, A., 2018. Geodynamic Gamechangers in Petroleum System Models. In 80th EAGE Conference and Exhibition 2018. https://doi.org/10.3997/2214-4609.201801042.

Hendricks, B.W.H., 2003. *Cooling and denudation of the Norwegian and Barents Sea Margins, Northern Scandinavia*. PhD thesis, Vrije Universiteit Amsterdam.

Hendriks, B.W.H., Andriessen, P.A.M., 2002. Pattern and timing of the post-Caledonian denudation of northern Scandinavia constrained by apatite fission track thermochronology. In: Doré, A.G., Cartwright, J.A., Stoker, M.S., Turner, J.P. and White, N.J. (Eds) Exhumation of the North Atlantic Margin: Timing, Mechanisms and Implications for Petroleum Exploration. Geological Society, London, Special Publications, 196, 117–137. https://doi.org/10.1144/GSL.SP.2002.196.01.08.

Hantschel, T., Kauerauf, A.I., 2009. Fundamentals of basin and petroleum systems modeling. Springer Science and Business Media.

Henriksen, E., Bjørnseth, H.M., Hals, T.K., Heide, T., Kiryukhina, T., Klovjan, O.S., Larssen, G.B., Ryseth, A.E., Rønning, K., Sollid, K., Stoupakova, A., 2011a. Uplift and erosion of the greater Barents Sea: impact on prospectivity and petroleum systems. In: Spencer, A.M., Embry, A.F., Gautier, D.L., Stoupakova, A.V. and Sørensen, K. (Eds.). Arctic Petroleum Geology. Geological Society Memoir 35, London, pp. 271–281. https://doi.org/10.1144/M35.17.

Henriksen, E., Ryseth, A.E., Larssen, G.B., Heide, T., Rønning, K., Sollid, K., Stoupakova, A.V., 2011b. Tectonostratigraphy of the greater Barents Sea: implications for petroleum systems. In: Spencer, A.M., Embry, A.F., Gautier, D.L., Stoupakova, A.V., Sørensen, K. (Eds.). Arctic Petroleum Geology. Geological Society Memoir 35, London, pp. 163–195. https://doi.org/10.1144/M35.10.

Henriksen, E., Kvamme, L., Rydningen, T.A., 2021. Hammerfest Basin Composite Tectono-Sedimentary Element. In: Drachev, S. S., Brekke, H., Henriksen, E. and Moore, T. (eds) Sedimentary Successions of the Arctic Region and their Hydrocarbon Prospectivity. Geological Society, London, Memoirs, 57. https://doi.org/10.1144/M57-2017-23.

Henriksen, E, Ktenas, D., Nielsen, J.K., 2022. Finnmark Platform Composite Tectono-Sedimentary Element, Barents Sea. In: Drachev, S. S., Brekke, H., Henriksen, E. and Moore, T. (eds) Sedimentary Successions of the Arctic Region and their Hydrocarbon Prospectivity. Geological Society, London, Memoirs, 57. https://doi.org/10.1144/M57-2020-20.

Jakobsson, M., Macnab, R., Mayer, L., Anderson, R., Edwards, M., Hatzky, J., Schenke, H.W., Johnson, P., 2008. An improved bathymetric portrayal of the Arctic Ocean: implications for ocean modelling and geological, geophysical and oceanographic analyses. Geophysical Research Letters, 35. https://doi.org/10.1029/2008GL033520.

Japsen, P., 2000. Investigation of multi-phase erosion using reconstructed shale trends based on sonic data. Sole Pit axis, North Sea. Global Planetary Change 24, 189–210. https://doi.org/10.1016/S0921-8181(00)00008-4.

Johansen, S.E., Ostisty, B. K., Fedorovsky, Y.F., Martirosjan, V.N., Christensen, O.B., Cheredeev, S.I., Ignatenko, E.A., Margulis, L.S., 1993. Hydrocarbon potential in the Barents Sea region: play distribution and potential. In Norwegian Petroleum Society Special

Publications (Vol. 2, pp. 273–320). Elsevier. https://doi.org/10.1016/B978-0-444-88943-0.50024-1.

Justwan, H., Dahl, B., 2005. Quantitative hydrocarbon potential mapping and organofacies study in the Greater Balder Area, Norwegian North Sea. In: Doré, A.G., Vining, B. (Eds.) Petroleum Geology: North-West Europe and Global Perspectives – Proceedings of the 6th Petroleum Geology Conference. Geological Society, London, 1317–1329. https://doi.org/10.1144/0061317.

Justwan, H., Dahl, B., Isaksen, G.H., 2006. Geochemical characterisation and genetic origin of oils and condensates in the South Viking Graben, Norway. Marine and Petroleum Geology 23(2), 213–239. https://doi.org/10.1016/j.marpetgeo.2005.07.003.

Killops, S., Stoddart, D., Mills, N., 2014. Inferences for sources of oils from the Norwegian Barents Sea using statistical analysis of biomarkers. Organic Geochemistry 76, 157–166.

Kishankov, A., Serov, P., Bünz, S., Patton, H., Hubbard, A.L., Mattingsdal, R., Vadakkepuliyambatta, S., Andreassen, K., 2022. Hydrocarbon leakage driven by quaternary glaciations in the Barents Sea based on 2D basin and petroleum system modeling. Marine and Petroleum Geology, 105557. https://doi.org/10.1016/j.marpetgeo.2022.105557.

Kjennerud, T., Sylta, Ø., 2001. Application of quantitative palaeobathymetry in basin modelling, with reference to the northern North Sea. Petroleum Geoscience 7(4), 331–341. https://doi.org/10.1144/petgeo.7.4.331.

Klausen, T.G., Müller, R., Sláma, J., Olaussen, S., Rismyhr, B., Helland-Hansen, W., 2017. Depositional history of a condensed shallow marine reservoir succession: stratigraphy and detrital zircon geochronology of the Jurassic Stø Formation, Barents Sea. Journal of the Geological Society 175, 130–145. https://doi.org/10.1144/jgs2017-024.

Knies, J., Matthiessen, J., Vogt, C., Laberg, J.S., Hjelstuen, B.O., Smelror, M., Larsen, E., Andreassen, K., Eidvin, T., Vorren, T.O., 2009. The Plio-Pleistocene glaciation of the Barents Sea-Svalbard region: a new model based on revised chronostratigraphy. Quaternary Science Reviews 28, 812–829. https://doi.org/10.1016/j.quascirev.2008.12.002.

Knies, J., Mattingsdal, R., Fabian, K., Grøsfjeld, K., Baranwal, S., Husum, K., Schepper, S.D., Vogt, C., Andersen, N., Matthiessen, J., Andreassen, K., Jokat, W., Nam, S., Gaina, C., 2014. Effect of early Pliocene uplift on late Pliocene cooling in the Arctic-Atlantic gateway. Earth and Planetary Science Letters 387, 132–144. https://doi.org/10.1016/j.epsl.2013.11.007.

Ktenas, D., Henriksen, E., Meisingset, I., Nielsen, J.K., Andreassen, K., 2017. Quantification of the magnitude of net erosion in the southwest Barents Sea using sonic velocities and compaction trends in shales and sandstones. Marine and Petroleum Geology 88, 826–844. https://doi.org/10.1016/j.marpetgeo.2017.09.019.

Ktenas, D., Meisingset, I., Henriksen, E., Nielsen, J.K., 2019. Estimation of net apparent erosion in the SW Barents Sea by applying velocity inversion analysis. Petroleum Geoscience 25 (2), 169–187. https://doi.org/10.1144/petgeo2018-002.

Lasabuda, A., Laberg, J.S., Knutsen, S.M., Høgseth, G., 2018. Early to middle Cenozoic paleoenvironment and erosion estimates of the southwestern Barents Sea: Insights from a regional mass-balance approach. Marine and Petroleum Geology 96, 501–521. https://doi.org/10.1016/j.marpetgeo.2018.05.039.

Lasabuda, A.P., Johansen, N.S., Laberg, J.S., Faleide, J.I., Senger, K., Rydningen, T.A., Patton H., Knutsen S.M., Hanssen, A., 2021. Cenozoic uplift and erosion of the Norwegian Barents Shelf–A review. Earth-Science Reviews, 217, 103609. https://doi.org/10.1016/j.earscirev.2021.103609.

Laberg, J.S., Andreassen, K. and Vorren, T.O., 2012. Late Cenozoic erosion of the high-latitude southwestern Barents Sea shelf revisited. Bulletin of Geological Society of America 124, 77–88. https://doi.org/10.1130/B30340.1.

Larssen, G.B., Elvebakk, G., Henriksen, L.B., Kristensen, S.E., Nilsson, I., Samuelsberg, T.J., Stemmerik, L., Worsley, D., 2005. Upper Palaeozoic Lithostratigraphy of the Southern Norwegian Barents Sea. Geological Survey of Norway Bulletin 444, 3–43.

Lerch, B., Karlsen, D.A., Matapour, Z., Seland, R., Backer-Owe, K., 2016. Organic geochemistry of Barents Sea petroleum: thermal maturity and alteration and mixing processes in oils and condensates. Journal of Petroleum Geology 39, 125–148. https://doi.org/10.1111/jpg.12637.

Lerch, B., Karlsen, D.A., Seland, R., Backer-Owe, K., 2017. Depositional environment and age determination of oils and condensates from the Barents Sea. Petroleum Geoscience 23 (2), 190–209. https://doi.org/10.1144/petgeo2016-039.

Lundschien, B.A., Høy, T., Mørk, A., 2014. Triassic hydrocarbon potential in the Northern Barents Sea; integrating Svalbard and stratigraphic core data. Norwegian Petroleum Directorate Bulletin, 11, 3–20.

Iyer, K., Hartz, E.H., Schmid, D.W., 2021. Methods to Estimate Erosion in Sedimentary Basins. Journal of Petroleum Geology, 44(2), 121-144. https://doi.org/10.1111/jpg.12782.

Magoon, L.B., Dow, W.G., 1994. The petroleum system. In L.B. Magoon and W.G. Dow (Eds.) The Petroleum System – From Source to Trap. AAPG Memoir 60, 3–24.

Meisingset, I., Hubred, J., Krasova, D., 2018. High quality regional velocity modelling for depth conversion. Presented at the First EAGE/PESGB Workshop on Velocities, 22–23 February 2018, London, UK. https://doi.org/10.3997/2214-4609.201800009.

Nadeau, P.H., 2011. Earth's energy “Golden Zone”: a synthesis from mineralogical research. Clay Minerals 46(1), 1–24. https://doi.org/10.1180/claymin.2011.046.1.1.

Nadeau, P.H., 2016. Uplifted Arctic Margins: New Concepts and Consequences for Barents Sea Exploration. NPF Arctic Exploration – Understanding the Barents Sea potential, Tromsø, Norway, 31 May-2 June 2016. 10.13140/RG.2.1.1819.6246.

Nasuti, A., Roberts, D., Gernigon, L., 2015. Multiphase mafic dykes in the Caledonides of northern Finnmark revealed by a new high-resolution aeromagnetic dataset. Norwegian Journal of Geology 95, 285–297. http://dx.doi.org/10.17850/njg95-3-02.

Nielsen, J.K., Joppen, T., Eikelmann, I., Schenk, O., Samu, L., Ma, F., Koronful, N., Samuelsberg, T., Henriksen, E., 2013. Ice and its potential impact on temperature and pressure of petroleum systems: Examples from the Norwegian Barents Sea. AAPG Search and Discovery Article #90177, 3P Arctic, Polar Petroleum Potential Conference & Exhibition, Stavanger, Norway, October 15–18, 2013.

Nielsen, J.K., Joppen, T., Eikelmann, I., Schenk, O., Samu, L., Koronful, N., Ma, F., Samuelsberg, T., MacGregor, A., Henriksen, E., 2014. The effects of glaciations on the petroleum systems in the Norwegian Barents Sea. Schlumberger SIS Global Forum 15–17 April 2014, Palau de Congressos de Catalunya, Barcelona, Spain.

Nielsen, J.K., Ktenas, D., Henriksen, E., Holm, D.H., Kaikas, E., Samu, L., Samuelsberg, T., 2015. Impact of ice ages and tectonic activity on the petroleum systems of the western Barents Sea, 3P Arctic: The Polar Petroleum Potential Conference and Exhibition, American Association of Petroleum Geologists (AAPG). Stavanger, Norway, Abstr. 2015.

Nilsen, K.T., Vendeville, B.C., Johansen, J.T., 1995. Influence of regional tectonics on halokinesis in the Nordkapp Basin, Barents Sea, in Salt Tectonics: A Global Perspective,

AAPG Mem., vol. 65, edited by M. P. A. Jackson, D. G. Roberts, S. Snelson, pp. 413–436, AAPG, Tulsa.

Norwegian Interactive Offshore Stratigraphic Lexicon. NORLEX. http://www.nhm2.uio.no/norlex/ [date accessed, June 2017].

NPD, 2017. Geological Assessment of Petroleum Resources in Eastern Parts of Barents SeaNorth 2017. Norwegian Petroleum Directorate (NPD), Stavanger, Norway, https://www.npd.no/globalassets/1-npd/publikasjoner/rapporter-en/geologivurderingbhn-engelsk-lavoppl.pdf, ISBN 978-82-7257-232-6, pp. 39.

NPD, 2022a. The Norwegian Petroleum Directorate FactPages of Exploration wellbores [date accessed, June 2022].

NPD, 2022b. Barents Sea Structural Elements Map. Norwegian Petroleum Directorate, Stavanger, Norway, NPD FactMaps [date accessed, June 2022].

Novoselov, A., Bykova, E., Henriksen, E., 2018. Geological Uplift and Erosion-Impact on Reservoir Quality of Petroleum Systems in the Barents Sea. In: Saint Petersburg 2018. https://doi.org/10.3997/2214-4609.201800330.

Nyland, B., Jensen, L.N., Skagen, J., Skarpnes, O., Vorren, T., 1992. Tertiary uplift and erosion in the Barents Sea: magnitude, timing and consequences. In: Larsen, R.M., Brekke, H., Larsen, B.T., Talleraas, E. (Eds). Structural and Tectonic Modelling and its Application to Petroleum Geology. Norwegian Petroleum Society, NPF Special Publication, 1, Elsevier, Amsterdam, pp. 153–162. https://doi.org/10.1016/B978-0-444-88607-1.50015-2.

Ohm, S.E., Karlsen, D.A., Austin, T.J.F., 2008. Geochemically driven exploration models in uplifted areas: example from the Norwegian Barents Sea. AAPG Bulletin 92, 1191–1223. https://doi.org/10.1306/06180808028.

Ostanin, I., Anka, Z., di Primio, R., 2017. Role of faults in hydrocarbon leakage in the Hammerfest Basin, SW Barents Sea: insights from seismic data and numerical modelling. Geosciences 2017 (7), 28. https://doi.org/10.3390/geosciences7020028.

Pascal, C., 2015. Heat flow of Norway and its continental shelf. Marine and Petroleum Geology 66, 956–969. https://doi.org/10.1016/j.marpetgeo.2015.08.006.

Pepper, A.S., Corvi, P.J., 1995. Simple kinetic models of petroleum formation. Part I: oil and gas from kerogen. Marine and Petroleum Geology 12, 291–319. https://doi.org/10.1016/0264-8172(95)98381-E.

Petersen, H.I., Nytoft, H.P., Vosgerau, H., Andersen, C., Bojesen-Koefoed, J.A., Mathiesen, A., 2010. Source rock quality and maturity and oil types in the NW Danish Central Graben: implications for petroleum prospectivity evaluation in an Upper Jurassic sandstone play area. In: Vining, B.A., Pickering, S.C. (Eds.) Petroleum Geology: From Mature Basins to New Frontiers – Proceedings of the 7th Petroleum Geology Conference. Geological Society, London, 95–111. https://doi.org/10.1144/0070095.

Rafaelsen. B., Andreassen, K., Hokstad, K., Kuilman, L.W., 2007. Large-scale glaciotectonic-imbricated thrust sheets on three-dimensional seismic data: facts or artefacts. Basin Research 19, 87–103. https://doi.org/10.1111/j.1365-2117.2007.00313.x.

Rasmussen, E., Fjeldskaar, W., 1996. Quantification of the Pliocene-Pleistocene erosion of the Barents Sea from present-day bathymetry. Global Planetary Change 12, 119–133. https://doi.org/10.1016/0921-8181(95)00015-1.

Riis, F., Fjeldskaar, W., 1992. On the magnitude of the late Tertiary and Quaternary erosion and its significance for the uplift of Scandinavia and the Barents Sea. In: Larsen, R.M., Brekke, H., Larsen, B.T., Talleraas, E. (Eds.), Structural and Tectonic Modelling and its

Application to Petroleum Geology. Norwegian Petroleum Society. Elsevier, pp. 163–185. https://doi.org/10.1016/B978-0-444-88607-1.50016-4.

Roberts, D., 2003. The Scandinavian Caledonides; event chronology, Palaeogeographic settings and likely modern analogues. Tectonophysics 365, 283–299. https://doi.org/10.1016/S0040-1951(03)00026-X.

Roberts, G., Christoffersen, T., 2018. Offshore Madagascar Part II: The Golden Zone. Geo ExPro, VXX, No X, February 2018.

Rojo, L.A., Cardozo, N., Escalona, A., Koyi, H., 2019. Structural style and evolution of the Nordkapp Basin, Norwegian Barents Sea. AAPG Bulletin 103(9), 2177-2217. https://doi.org/10.1306/01301918028.

Ryseth, A., Augustson, J.H., Charnock, M., Haugerud, O., Knutsen, S.M., Midbøe, P.S., Opsal, J.G., Sundsbø, G., 2003. Cenozoic stratigraphy and evolution of the Sørvestsnaget Basin, southwestern Barents Sea. Norsk Geologisk Tidsskrift 83, 107–130.

Smelror, M., Petrov, O.V., Larssen, G.B., Werner, S.C., 2009. Geological history of the Barents Sea. Norges Geologisk undersøkelse, 1–135.

Spencer, A.M., Embry, A.F., Gautier, D.L., Stoupakova, A.V., Sørensen, K., 2011. An overview of the petroleum geology of the Arctic. Geological Society, London, Memoirs 35(1), 1–15. https://doi.org/10.1144/M35.1.

Stemmerik, L., Worsley, D., 2005. 30 years on: Arctic Upper Palaeozoic stratigraphy, depositional evolution and hydrocarbon prospectivity. Norwegian Journal of Geology 85, 151–168.

Sweeney, J.J., Burnham, A.K., 1990. Evaluation of a simple model of vitrinite reflectance based on chemical kinetics (1). AAPG bulletin 74(10), 1559–1570.

https://doi.org/10.1306/0C9B251F-1710-11D7-8645000102C1865D.

Walderhaug, O., 1996. Kinetic modelling of quartz cementation and porosity loss in deeply buried sandstones reservoirs. AAPG Bulletin 80, 731–745. https://doi.org/10.1306/64ED88A4-1724-11D7-8645000102C1865D.

Walderhaug, O., 2000a. Modeling quartz cementation and porosity in Middle Jurassic Brent Group sandstones of the Kvitebjørn Field, northern North Sea. AAPG Bulletin 84(9), 1325–1339. https://doi.org/10.1306/A9673E96-1738-11D7-8645000102C1865D.

Walderhaug, O., Lander, R.H., Bjørkum, P.A., Oelkers E.H., Bjørlykke, K., Nadeau, P.H., 2000b. Modeling of quartz cementation and porosity in reservoir sandstones: Examples from the Norwegian Continental Shelf. In: R. Wordern (Ed.) Quartz cementation: International Association of Sedimentology, Spec. Vol. 29, 39–49. https://doi.org/10.1002/9781444304237.ch3.

Walderhaug, O., Bjørkum, P.A., 2003. The effect of stylolite spacing on quartz cementation in the Lower Jurassic Stø Formation, southern Barents Sea. Journal of Sedimentary Research 73(2), 146–156. https://doi.org/10.1306/090502730146.

Welte, D.H., Horsfield, B., Baker, D.R. (Eds.)., 2012. Petroleum and basin evolution: Insights from petroleum geochemistry, geology and basin modeling. Springer Science & Business Media.

Wenger, L. M., Davis, C. L., Isaksen, G. H., 2002. Multiple controls on petroleum biodegradation and impact on oil quality. SPE Reservoir Evaluation & Engineering, 375–383. https://doi.org/10.2118/80168-PA.

Wilhelms, A., Larter, S.R., Head, I., Farrimond, P., Di Primio, R., Zwach, C., 2001.

Biodegradation of oil in uplifted basins prevented by deep-burial sterilization. Nature [London] 411, 1034-1037. https://doi.org/10.1038/35082535.

Wygrala, B.P., 1989. *Integrated study of an oil field in the southern Po basin, northern Italy*. PhD thesis, Köln University, Jülich Research Centre, Jülich, Germany.

Tasianas, A., Bünz, S., Bellwald, B., Hammer, Ø., Planke, S., Lebedeva-Ivanova, N., Krassakis, P., 2018. High-resolution 3D seismic study of pockmarks and shallow fluid flow systems at the Snøhvit hydrocarbon field in the SW Barents Sea. Marine Geology, 403, 247–261. https://doi.org/10.1016/j.margeo.2018.06.012.

Torsvik, T.H., Van der Voo, R., Meert, J.G., Mosar, J., Walderhaug, H.J., 2001. Reconstructions of the continents around the North Atlantic at about the 60th parallel. Earth Planetary Science Letters 187(1-2), 55–69. https://doi.org/10.1016/S0012-821X(01)00284-9.

Tissot, B.P., Welte, D.H., 1984. Petroleum formation and occurrence. Springer-Verlag Berlin, Heidelberg, pp. 702.

Tsikalas, F., Faleide, J.I., Eldholm, O., Blaich, O.A., 2012. The NE Atlantic conjugate margins. Regional Geology and Tectonics: Phanerozoic Passive Margins, Cratonic Basins and Global Tectonic Maps, 140–201. Doi 10.1016/B978-0-444-56357-6.00004-4.

Van Koeverden, J.H., D.A. Karlsen, Schwark, L., Chpitsglouz, A., Backer-Owe, K., 2010. Oil-prone Lower Carboniferous coals in the Norwegian Barents Sea. Implications for a Paleozoic petroleum system. Journal of Petroleum Geology 33, 155–182. https://doi.org/10.1111/j.1747-5457.2010.00471.x.

Vorren, T.O., Richardsen, G., Knutsen, S.M., Henriksen, E., 1991. Cenozoic erosion and sedimentation in the western Barents Sea. Marine and Petroleum Geology 8, 317–340. https://doi.org/10.1016/0264-8172(91)90086-G.

Zattin, M., Andreucci, B., de Toffoli, B., Grigo, D., Tsikalas, F., 2016. Thermochronological constraints to late Cenozoic exhumation of the Barents Sea Shelf. Marine and Petroleum Geology 73, 97–104. https://doi.org/10.1016/j.marpetgeo.2016.03.004.

Zieba, K. J., Grøver, A., 2016. Isostatic response to glacial erosion, deposition and ice loading. Impact on hydrocarbon traps of the southwestern Barents Sea. Marine and Petroleum Geology 78, 168–183. https://doi.org/10.1016/j.marpetgeo.2016.09.009.

Figure captions:

Figure 1. Map of the Norwegian Barents Sea showing the different structural elements and oil-gas discoveries. The regional profiles A-A', B-B', C-C' and D-D' and the wells studied along the lines are indicated with a red colour and red dots, respectively. The location of the study area is indicated in the inserted figure. Modified from the Norwegian Petroleum Directorate (NPD, 2022b) and Jakobsson et al. (2008).

Figure 2. Tectonostratigraphic chart from the southwestern Barents Sea, showing petroleum system elements such as source rocks and reservoir rocks as well as major geodynamic events such as rifting phases and uplift-erosion events during tectonic and ice-age events. Modified

from Ohm et al. (2008) and the Norwegian Interactive Offshore Stratigraphic Lexicon (NORLEX).

Figure 3. The upper panel shows the interpreted seismic 2D profile A-A' passing from the Sørvestsnaget Basin, Loppa High, Hammerfest Basin and the Finnmark Platform illustrates the basin configuration, the changes in structural styles and geometries. Areas with missing sections and major erosion can be identified along the profile. The lower panel illustrates the 2D basin and petroleum systems model along the seismic 2D profile. For the location of the 2D line see Figure 1 (Modified after Ktenas et al., 2017).

Figure 4. Seismic Profile B-B' reaching across the Nysleppen Fault Complex and through the well 7124/3-1 (Bamse).

Figure 5. Seismic Profile C-C' reaching across the Nysleppen Fault Complex and through the wells 7125/1-1 (Binne) and 7125/4-1 (Nucula).

Figure 6. Seismic Profile D-D' reaching from the large diapirs in the southwestern Nordkapp Basin and onto the eastern part of the Finnmark Platform. The major unconformity of Plio-Pleistocene (URU) is truncating salt diapirs and the tilted layers on the Finnmark Platform.

Figure 7. Conceptual models for the estimation of net apparent erosion derived from the velocity inversion (sonic logs, seismic profiles and time structure grids) and vitrinite

reflectance. a) The net apparent erosion is estimated by matching the green sonic log against the blue and red curves representing Lower Jurassic-Upper Triassic sandstones and Cretaceous shales, respectively. b) The upper panel shows two layers of Cretaceous (green) and Lower Jurassic-Upper Triassic age (yellow) with their mid-points superimposed. The lower panel shows the calculation of the net apparent erosion, as the vertical depth difference between the layers' baseline, where the layers would have been at maximum depth of burial and the present depth of burial. c) Measurements of vitrinite reflectance (%Ro) represent the deepest burial depth and the thermal maturity of the sediments; however, where unexpectedly high values are encountered, this points to a deeper burial depth in the past followed by an uplift-erosion event. Modified after Ktenas et al. (2017; 2019).

Figure 8. Mechanisms affecting the depth and the temperature expected of the Golden Zone. On the left side of the figure, sedimentary deposits subjected to normal subsidence are reaching their maximum burial depth at present day, which is typically found for the North Sea, for example. On the right side of the figure, the major erosion events that characterise the Norwegian Barents Sea have shifted the hydrocarbon accumulation zone to a shallower depth and a lower temperature at present. Redrawn after Nadeau (2011; 2016).

Figure 9. Geological development along the 2D profile by back-stripping of the layers through geological time. Note that the back-stripping comprised de-compaction and integrated uplift-erosion events in 2D modelling. Examples, namely, pre-glaciation Age, Last Glacial Maximum and the present day are shown.

Figure 10. Qualitative maturity map showing oil and gas windows of the Hekkingen Formation at Base Cretaceous Unconformity (BCU) level, applying a regional net apparent erosion map from Ktenas et al. (2017) and Ktenas et al. (2019).

Figure 11. Maturity of source rocks along the 2D profile expressed as a) vitrinite reflectance EASY%Ro (Sweeney and Burnham, 1990) and b) a transformation ratio in percentage of kerogen to petroleum. c) The Critical Moment (TR=50%) is expressing the timing when the trap should be in place for a successful charge to occur, according to Magoon and Dow (1994). Note that the modelled source rocks are not necessarily continuously distributed along the whole 2D profile. Abbreviations of the source rocks: J: Upper Jurassic Hekkingen; Tr: Triassic Kobbe-Klappmyss; P: Permian Ørret; PP: Pre-Permian Tettegras.

Figure 12. Hydrocarbon zonation of a) kerogen Type II (B) and b) kerogen Type IIIH (DE) after Pepper and Corvi (1995), representing the present-day maturity of source rocks in terms of immature, oil, gas and overmature zones. The zonation is predominantly controlled by kinetics of the source rocks and the burial and thermal history. c) Expulsion onset showing when the source rocks began to expel oil and gas into adjacent rocks. Close-up of the 2D profile of the Hammerfest Basin, Nysleppen Fault Complex and Finnmark Platform. For the abbreviations of the source rocks see the caption to Figure 11.

Figure 13. The 2D profile of the Hammerfest Basin, Nysleppen Fault Complex and Finnmark Platform shows the transformation ratio of the source rocks at the present day. The locations of time extractions of the source rocks are shown along the section and within the inset. The time

extractions show the transformation of kerogen to petroleum and the EASY%Ro of Sweeney and Burnham (1990) for the Permian, Triassic and Upper Jurassic source rocks. Less mature source rocks are seen for the Finnmark Platform area compared with the basin areas. For the abbreviations of the source rocks see the caption to Figure 11.

Figure 14. Reservoir rocks. a) Their temperatures at the present day and b) maximum temperatures experienced through burial history. Note that these reservoir rocks are not necessarily evenly distributed along the 2D profile showing the Hammerfest Basin, Nysleppen Fault Complex and Finnmark Platform. Abbreviations of the reservoir rocks: J: Jurassic Tubåen, Nordmela and Stø; SF: Triassic Snadd and Fruholmen; KKU: Triassic Kobbe and Klappmyss Upper; KKL: Triassic Kobbe and Klappmyss Lower; PPU: Pre-Permian Upper; PPL: Pre-Permian Lower.

Figure 15. Effective porosity of reservoir rocks. Note that the reservoir rocks are not necessarily evenly distributed along the whole 2D profile. For the abbreviations of the reservoir rocks see the caption to Figure 14.

Figure 16. a) Chemical compaction and its related loss of porosity where the chemical compaction resulting from quartz cementation can be controlled by the amount of clay coatings on quartz grains as a function of grain size and the temperatures that the reservoir rock has experienced through time. b) Time extractions showing porosity loss in sandstones through time, which is derived from the Walderhaug Quartz Cementation Model (Walderhaug, 2000). Each of the time extractions illustrates various degree of grain coatings from 25, 50 and 75%

and its impact on cementation through time. The locations of the time extractions are indicated on the 2D profile. Note that the reservoir rocks are not necessarily evenly distributed along the whole 2D profile. Abbreviations of the reservoir rocks: J: Jurassic Tubåen, Nordmela and Stø; SF: Triassic Snadd and Fruholmen; KKU: Triassic Kobbe and Klappmyss Upper; KKL: Triassic Kobbe and Klappmyss Lower; PPU: Pre-Permian Upper; PPL: Pre-Permian Lower.

Figure 17. Depth-temperature cross plot for the southwestern Barents Sea This plot is showing down-hole and bottom-hole temperatures measured through DST and TD at the present day, based on data released by the NPD. The small black arrows illustrate how the maximum depth of burial ((derived from vitrinite reflectance and the estimates from Ktenas et al. (2017, 2019)) was shifted towards a shallower depth at the present-day due to tectonic and glacigenic uplift and erosion events. Note the grey dashed line separating down-hole temperatures (DST) in the upper part of the golden-reddish coloured field. The DST temperatures (except for one measurement point) suggest an approximate range of 35-100°C for reservoir targets in the Norwegian Barents Sea. DST measurements targeting reservoirs are all within the solid blue polygon, which in the study area is reflecting a lower temperature range for discoveries than the *sensu stricto* Golden Zone. Potentially, the blue dashed polygon indicates an extension towards even shallower depth and lower temperature range for the Golden Zone. Examples of Barents Sea discoveries: 1 – Well 7324/7-2 Hanssen oil discovery in the Stø Formation, 2 – Well 7122/7-2 Goliat oil discovery in the Tubåen Formation, 3 – Well 7121/7-1 Albatross gas/condensate discovery in the Stø Formation, 4 – Well 7226/11-1 gas discovery in the Havert Formation.

Highlights of the manuscript:

- Basin modelling (1D and 2D) has been performed for a selected number of wells and along one regional 2D seismic line by integrating net apparent erosion estimates for the southwestern Barents Sea. This has resulted in an assessment of the impact of maximum burial and net apparent erosion on the petroleum systems.

- Simulation results indicate that the Upper Jurassic source rock is immature to marginally mature in the central and eastern Norwegian Barents Sea. In contrast, the western part has very deeply buried Upper Jurassic Hekkingen source rock in the deepest Cretaceous grabens where it is in overmature or in dry gas-mature zones; on the flanks it has late oil to peak-oil maturity.

- The Permian Ørret, the Lower-Middle Triassic basal Klappmyss and basal Kobbe shales may be important gas-prone source rocks in the eastern Norwegian Barents Sea.

- As a consequence of the severe exhumation in the southwestern Barents Sea, it is important to adjust the exploration strategy to shallower depth and lower temperatures.

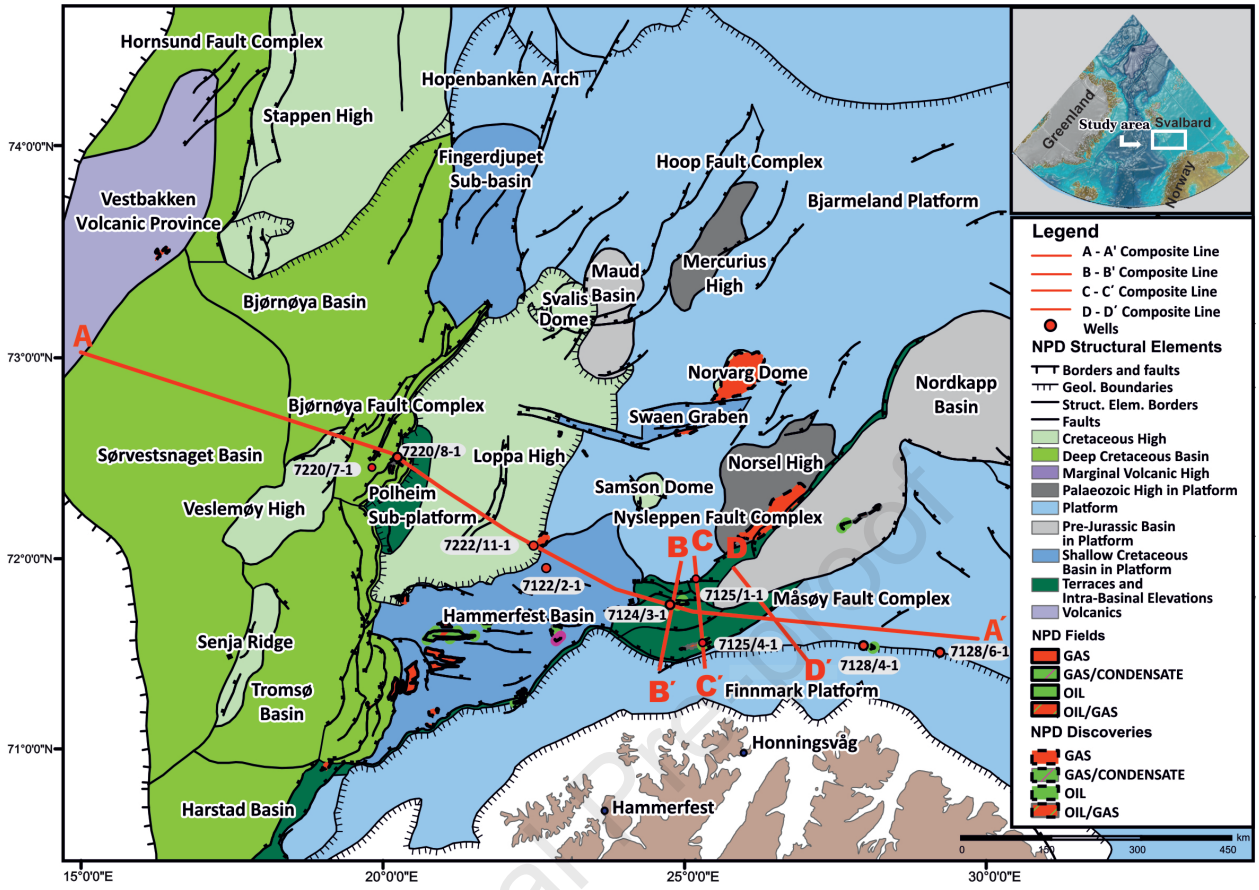

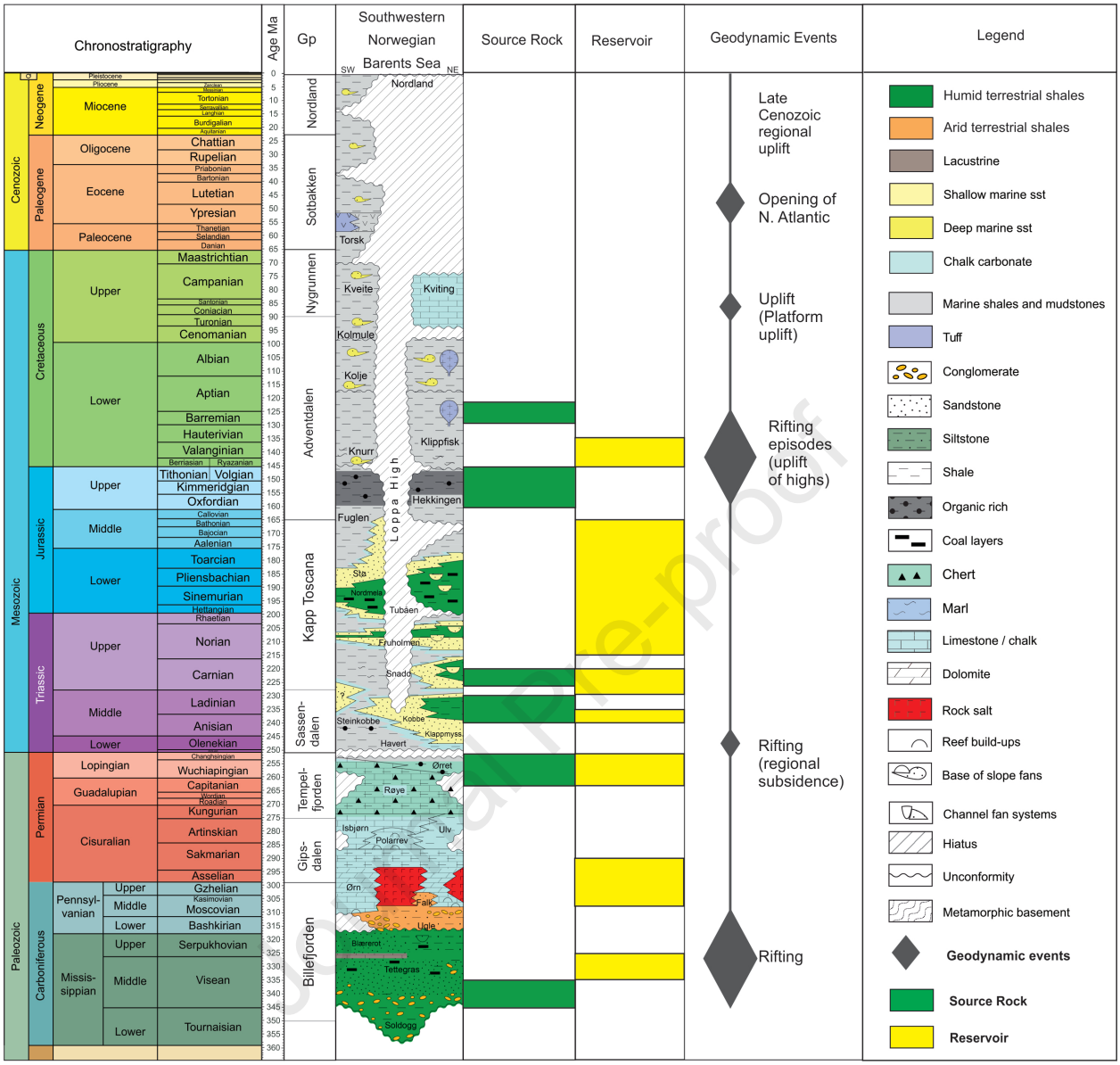

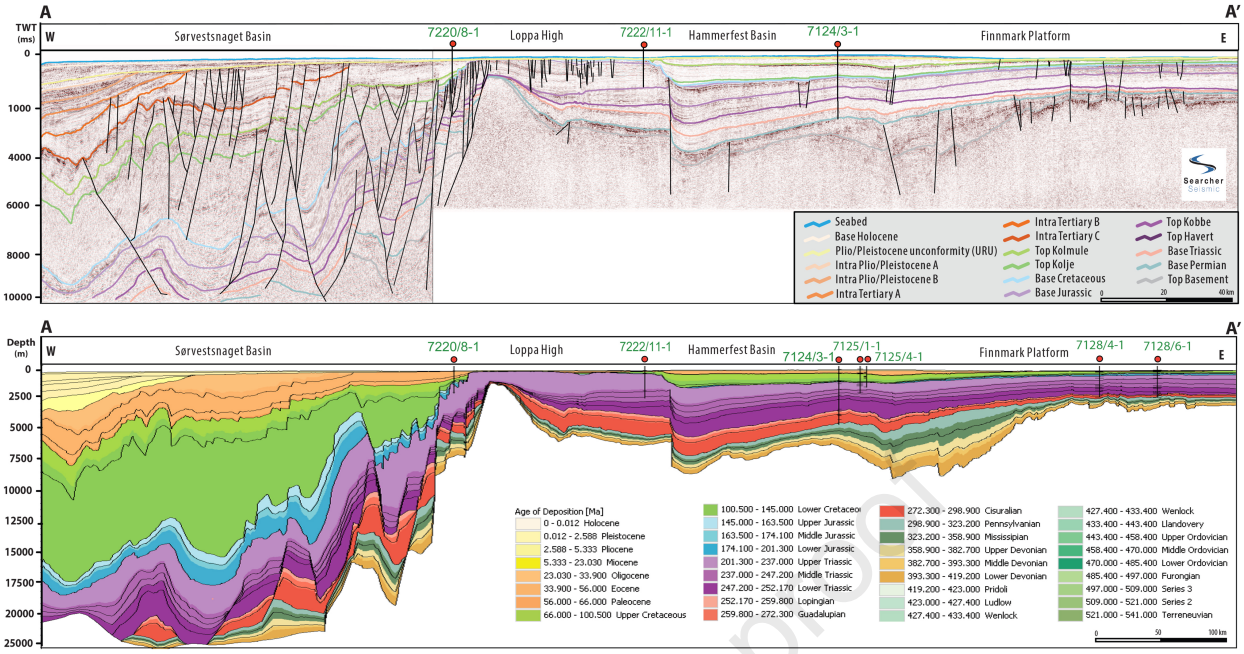

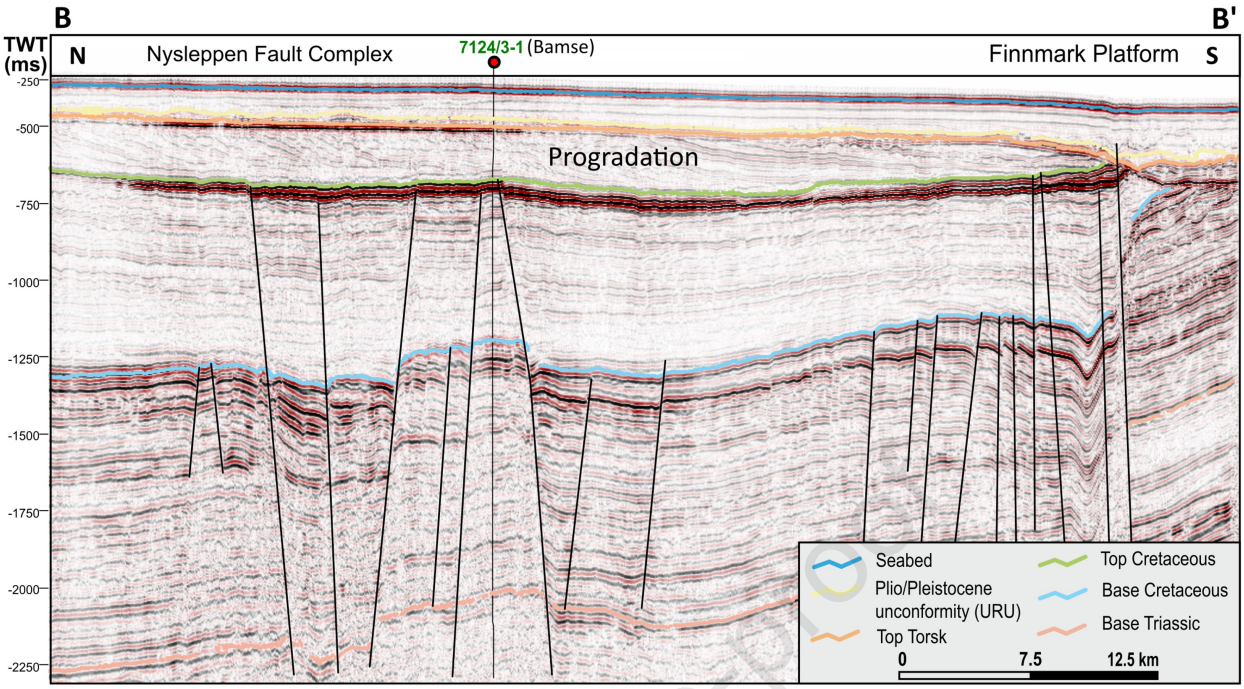

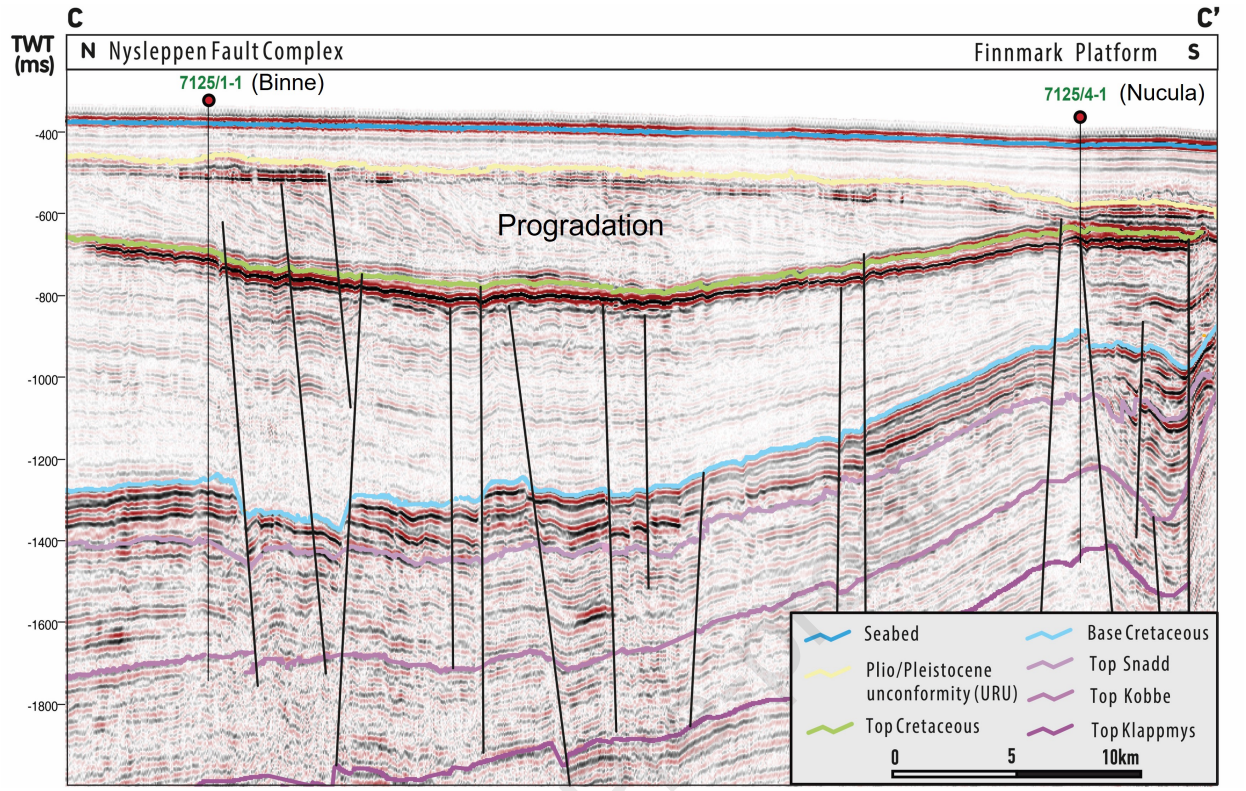

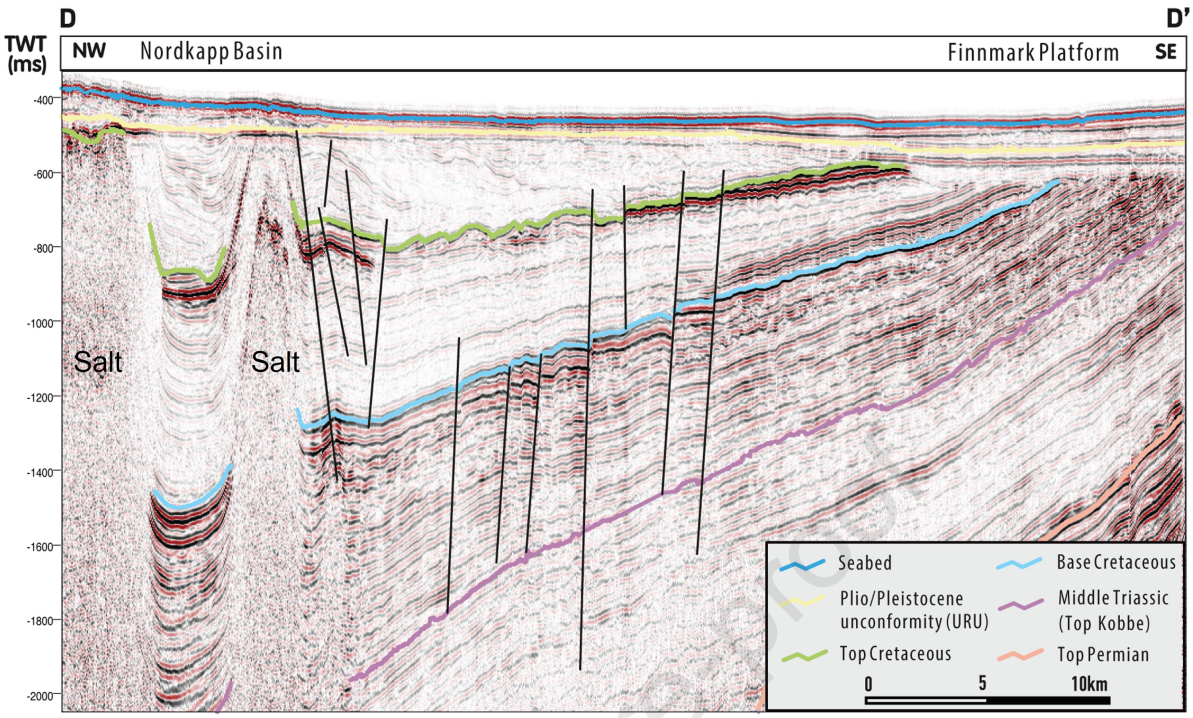

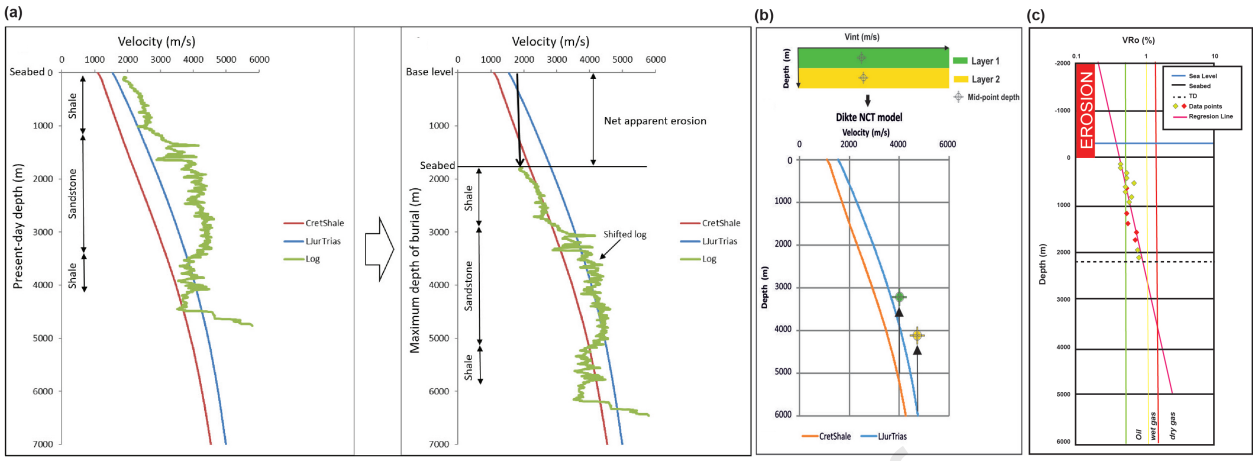

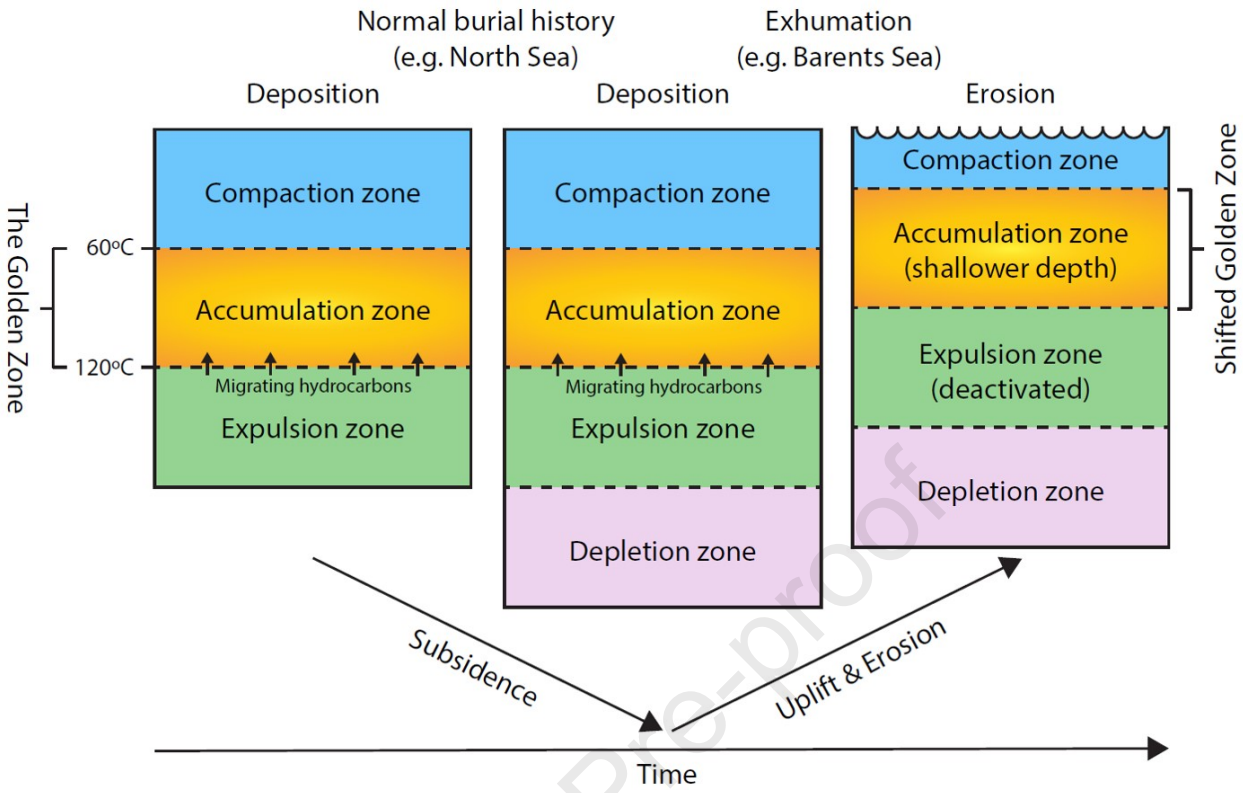

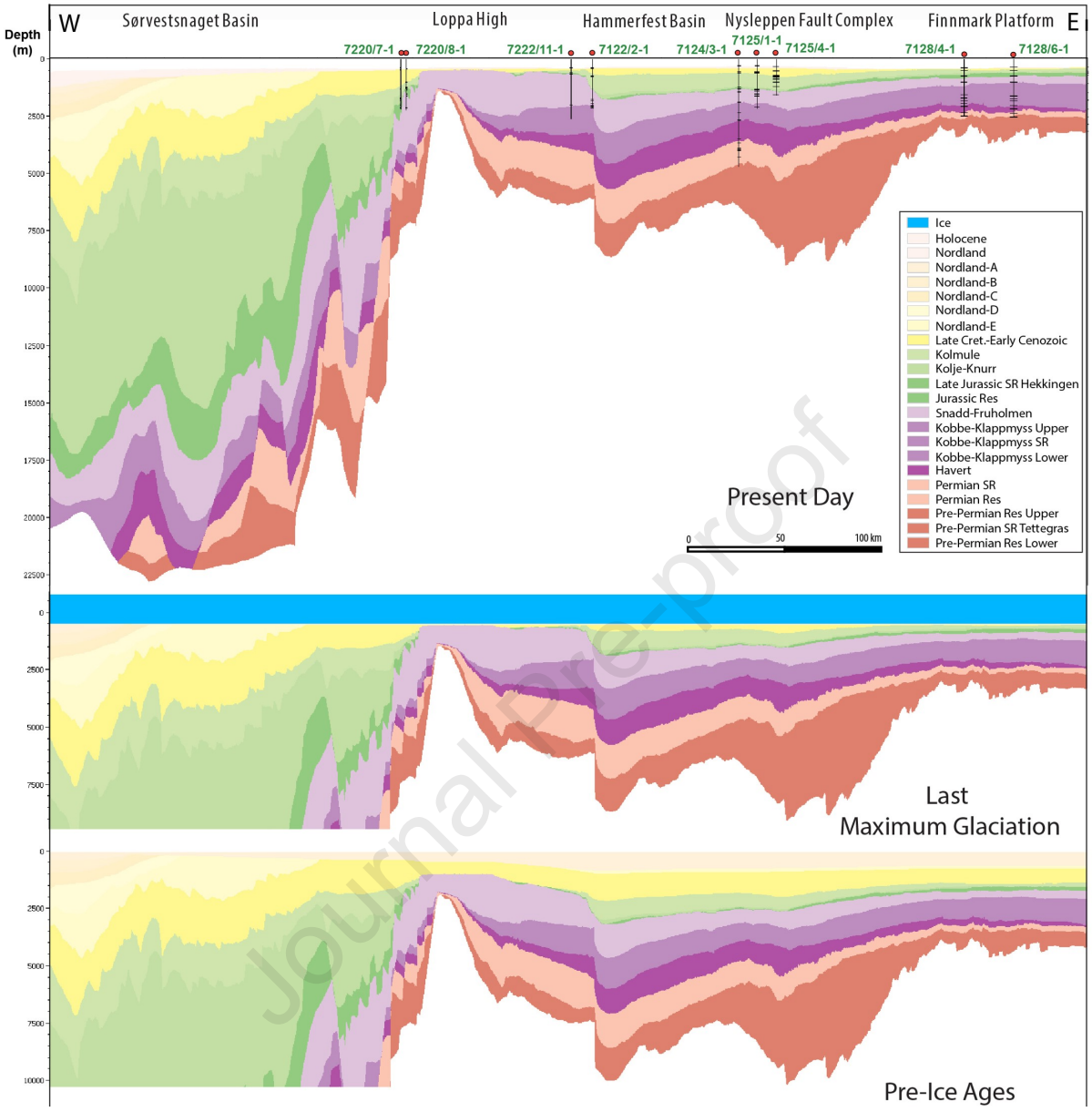

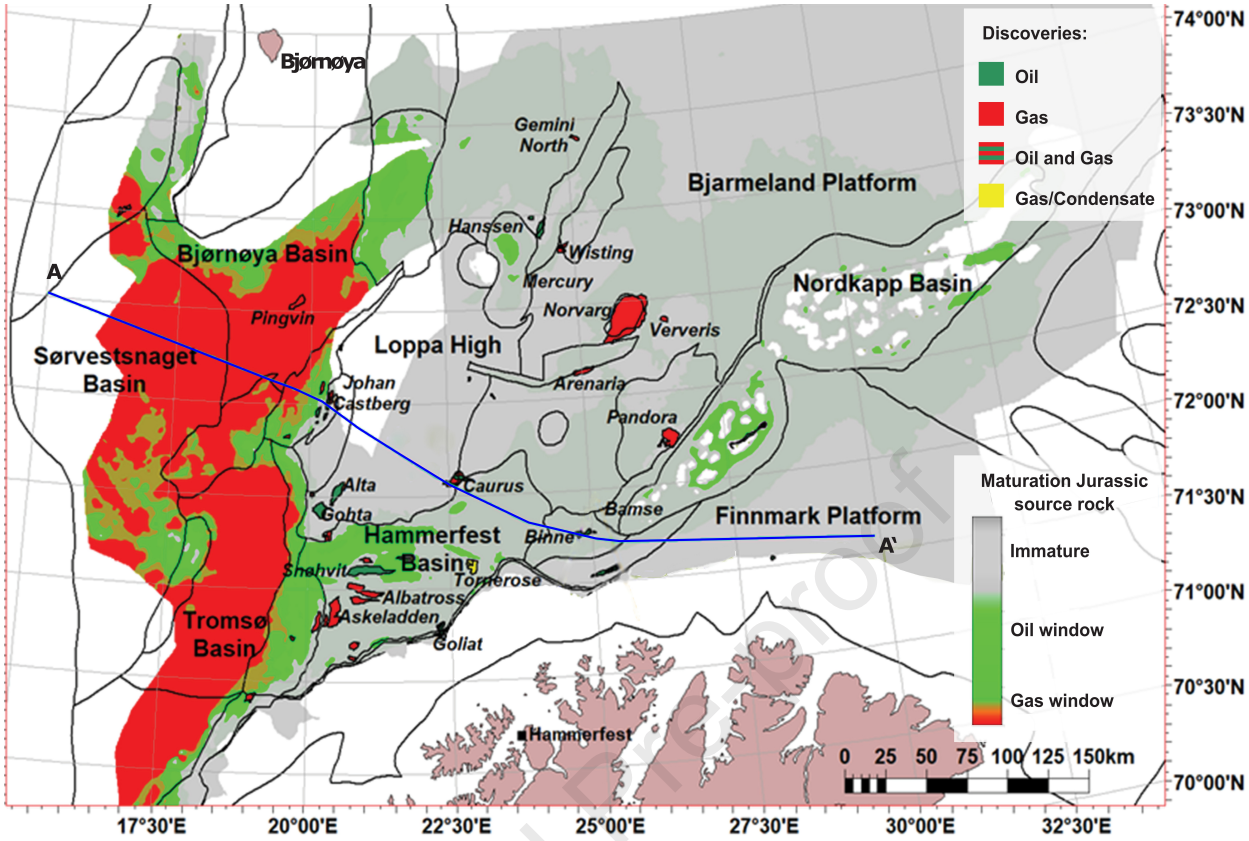

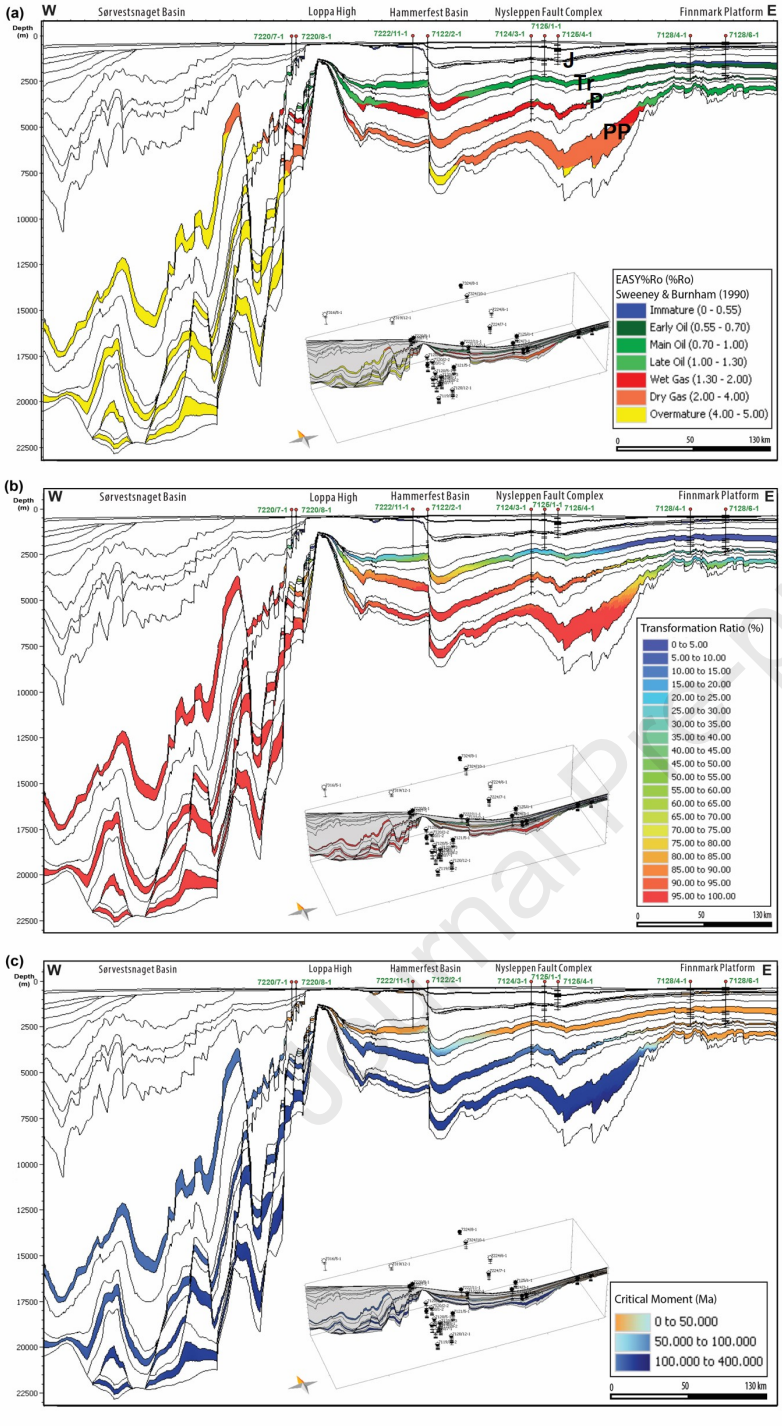

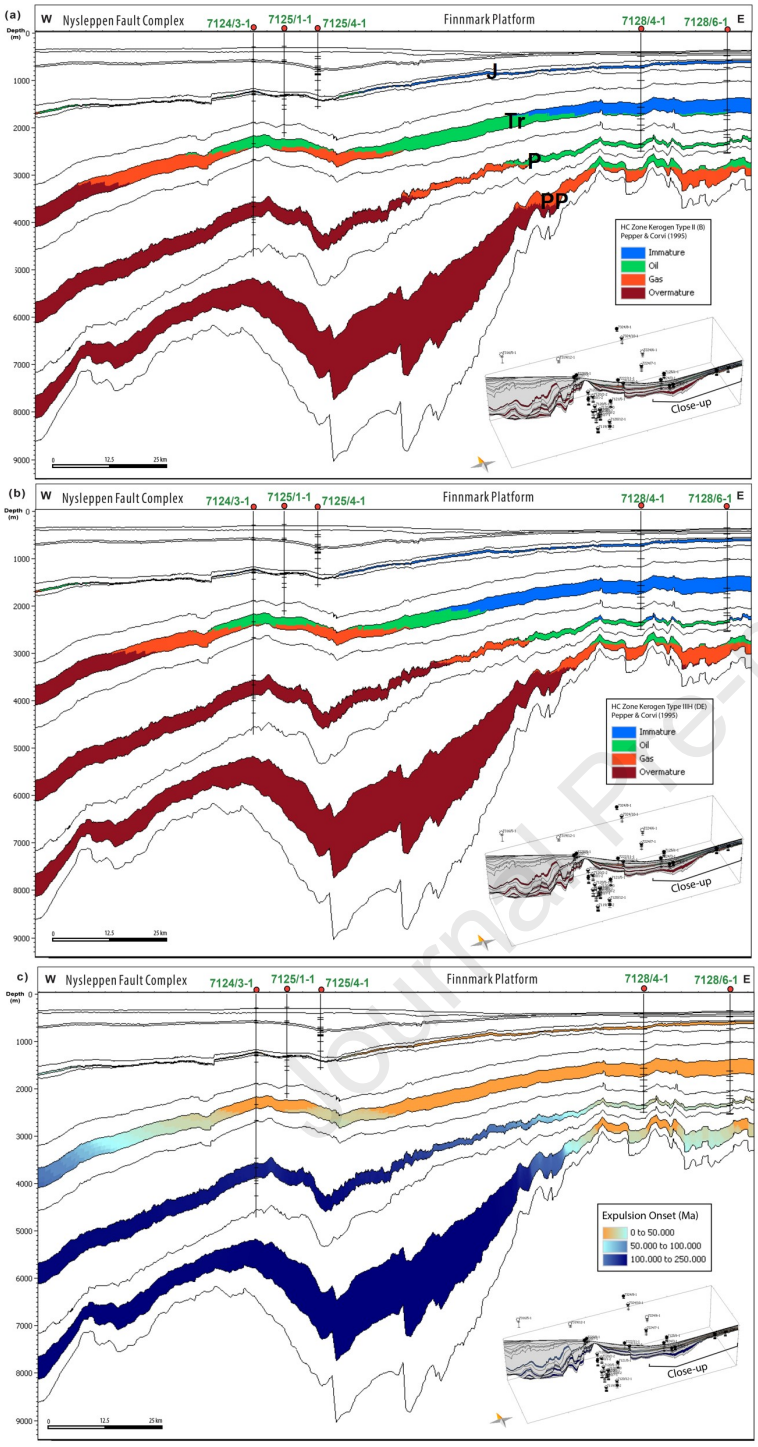

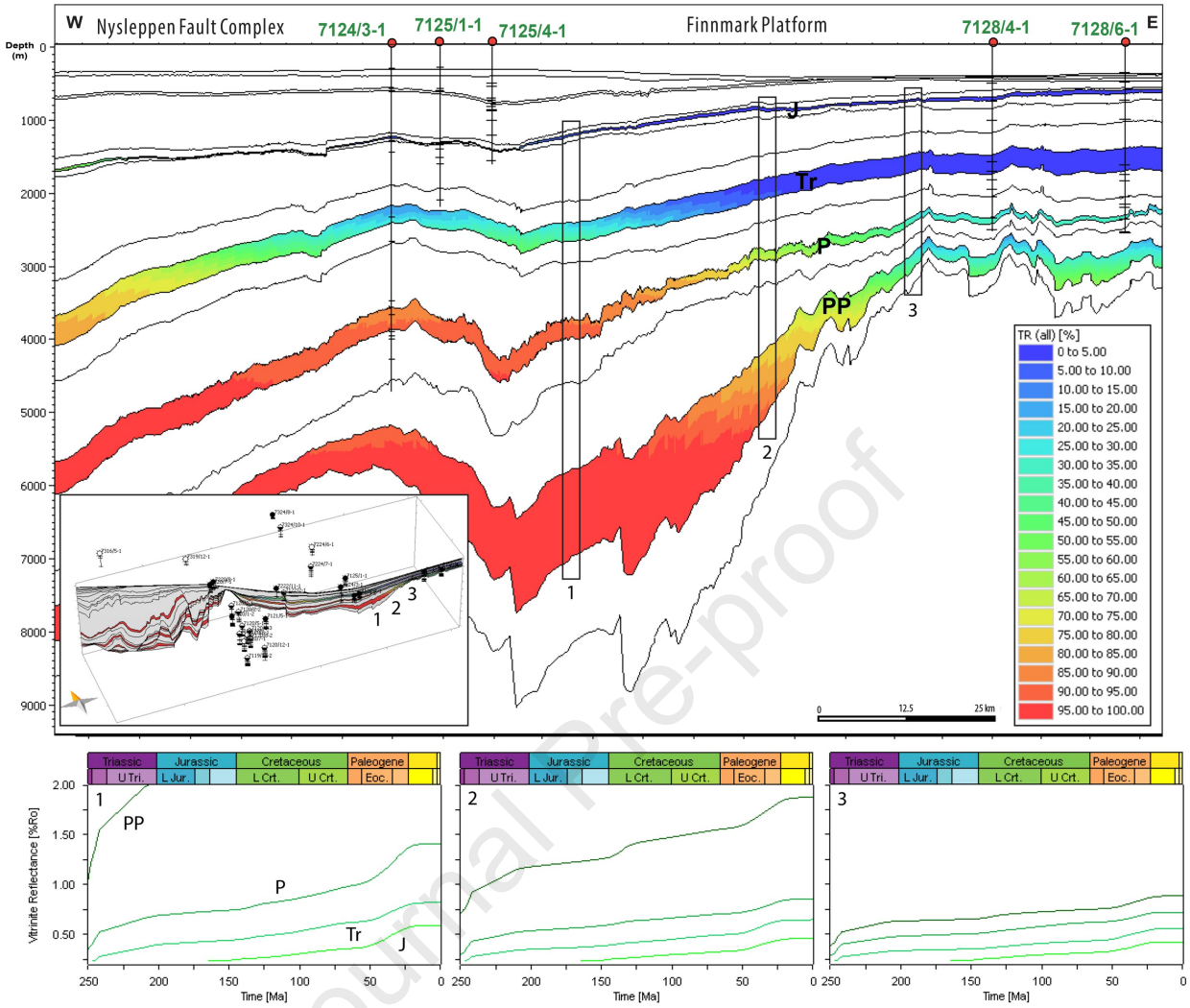

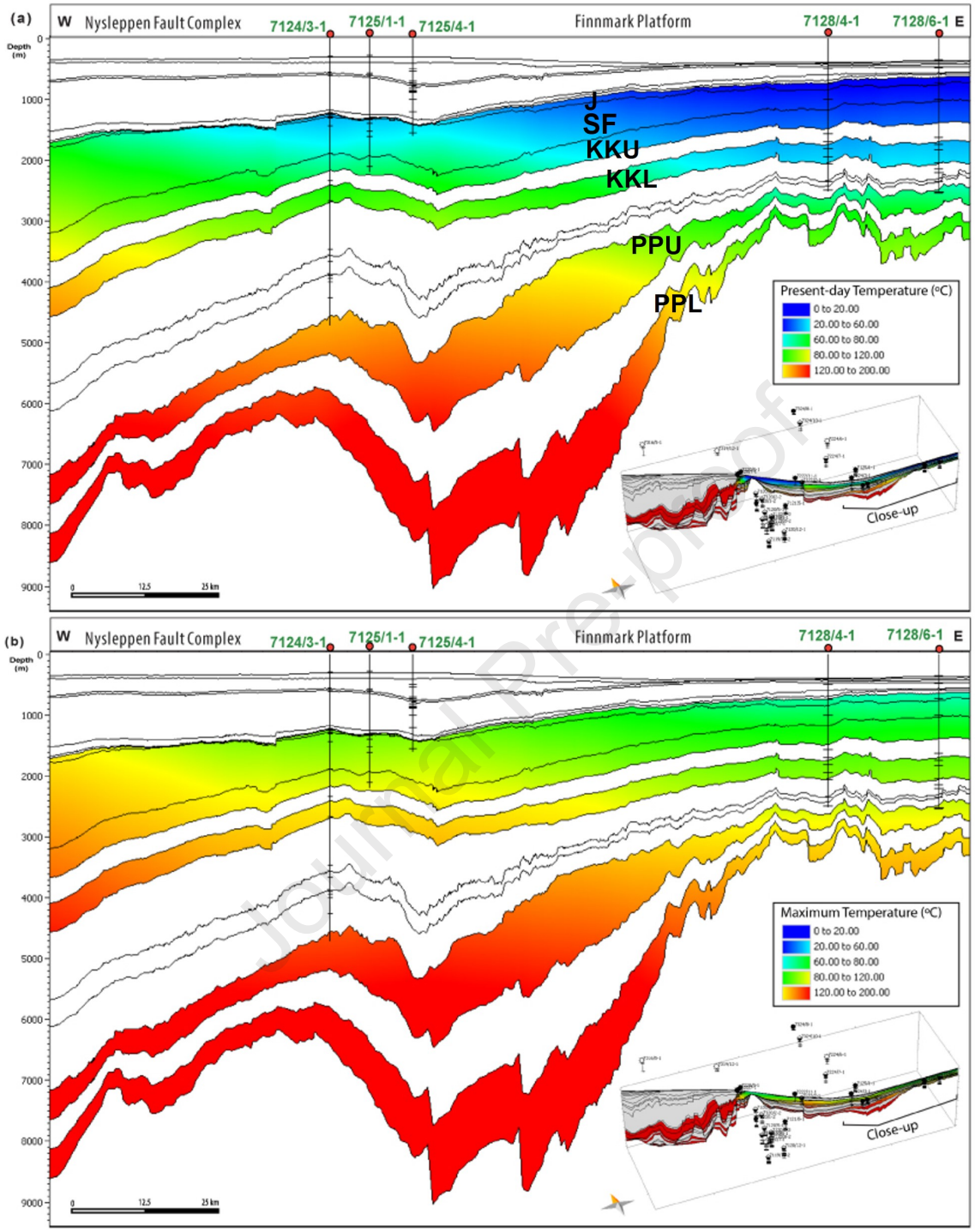

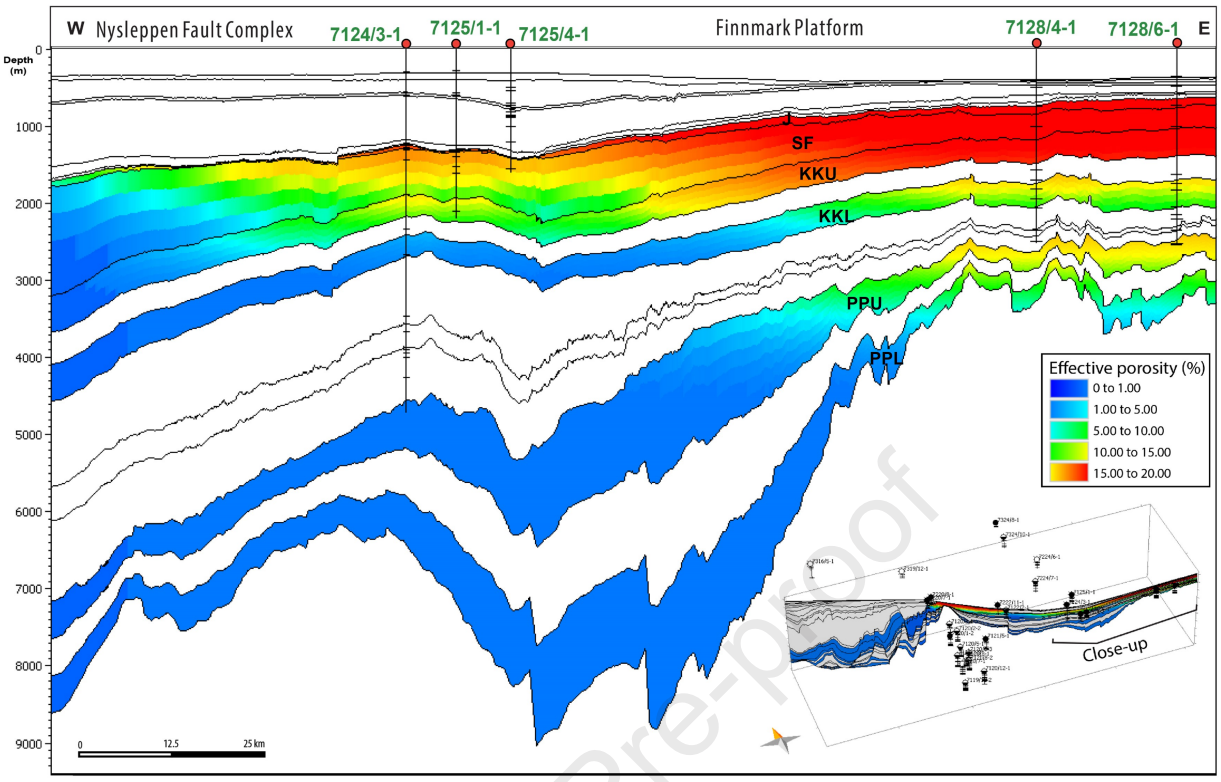

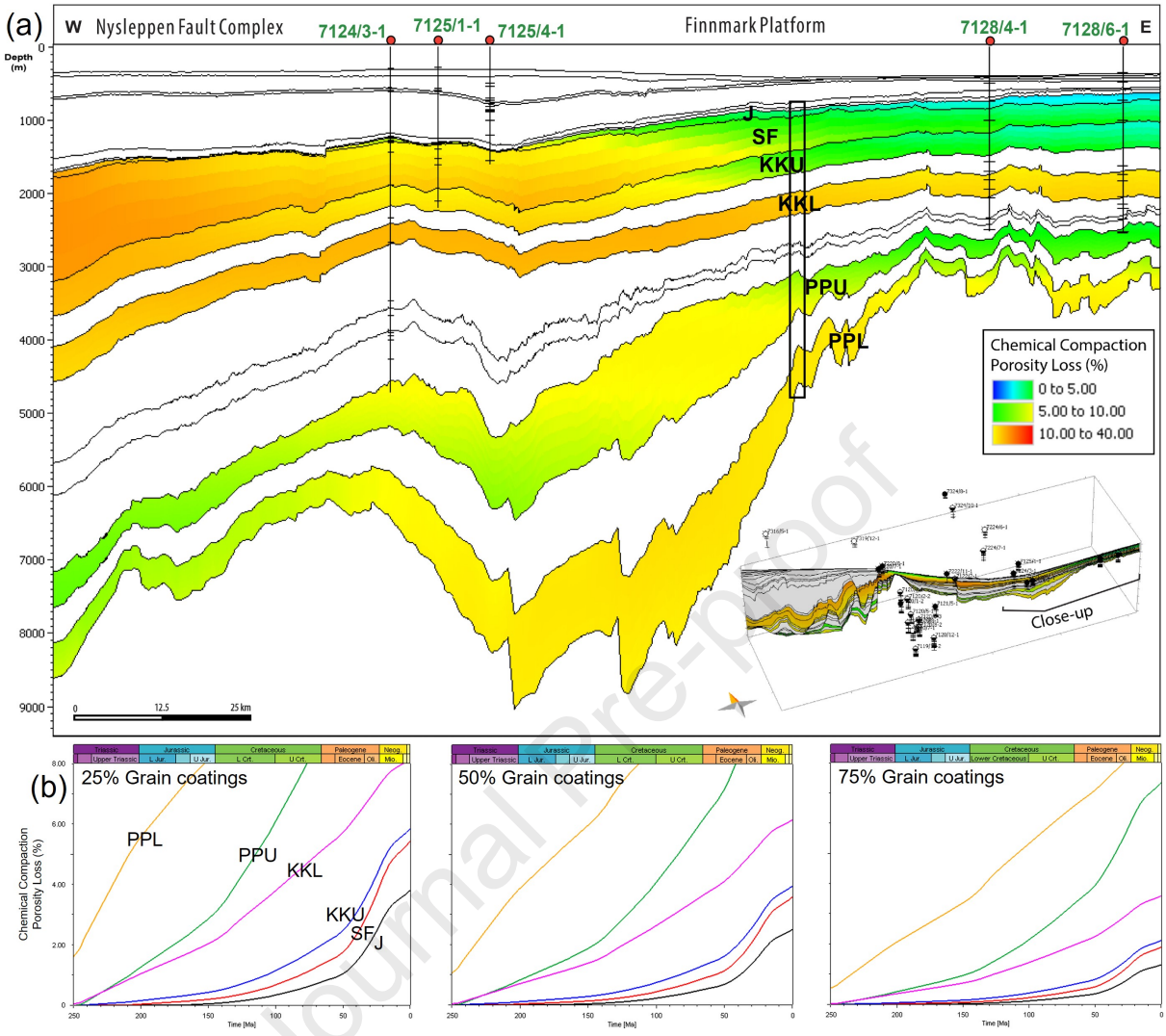

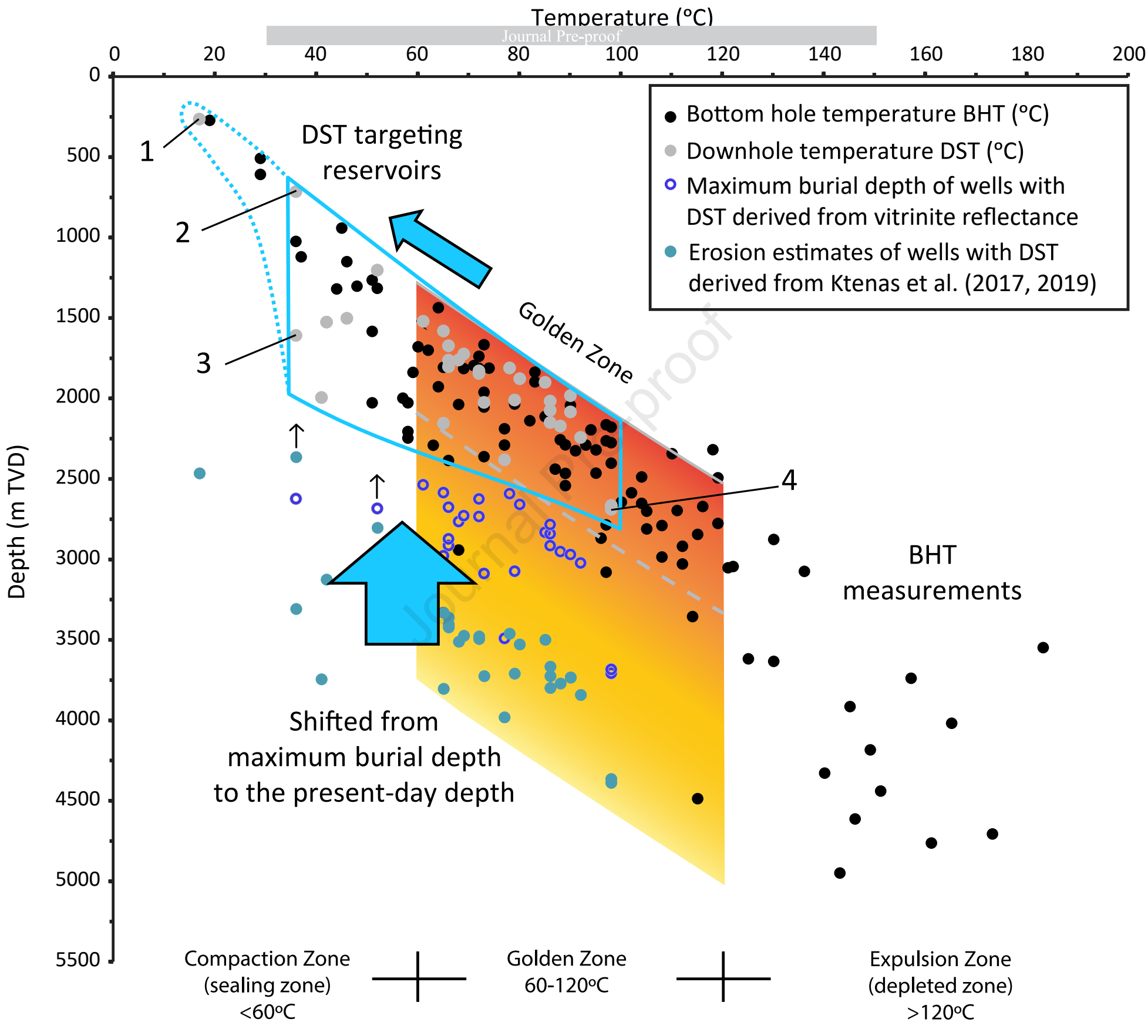
Temperature (°C)
Journal Pre-proof
0
20
40
60
80
100
120
140
160
180
200
Depth (m TVD)
0
500
1000
1500
2000
2500
3000
3500
4000
4500
5000
5500
Bottom hole temperature BHT (°C)
Downhole temperature DST (°C)
Maximum burial depth of wells with DST derived from vitrinite reflectance
Erosion estimates of wells with DST derived from Ktenas et al. (2017, 2019)
1
2
3
4
DST targeting reservoirs
Golden Zone
BHT measurements
Shifted from maximum burial depth to the present-day depth
Compaction Zone (sealing zone) <60°C
Golden Zone 60-120°C
Expulsion Zone (depleted zone) >120°C

Declaration of interests

☒ The authors declare that they have no known competing financial interests or personal relationships that could have appeared to influence the work reported in this paper.

☐The authors declare the following financial interests/personal relationships which may be considered as potential competing interests: